UNIVERSITÄTSKLINIKUM HAMBURG-EPPENDORF

Klinik und Poliklinik für Mund-, Kiefer- und Gesichtschirurgie

Univ.-Prof. Dr. med. Dr. med. dent. Martin Gosau

Antibacterial Properties of Functionalized Silk Fibroin and Sericin Membranes for Wound Healing Applications in Oral and Maxillofacial Surgery

Dissertation

zur Erlangung des Grades eines Doktors der Medizin
an der Medizinischen Fakultät der Universität Hamburg.

vorgelegt von:

Sogand Schäfer
aus Shiraz

Hamburg 2022

Angenommen von der
Medizinischen Fakultät der Universität Hamburg am: 30.01.2025

Veröffentlicht mit Genehmigung der
Medizinischen Fakultät der Universität Hamburg.

Prüfungsausschuss, der/die Vorsitzende: Prof. Dr. Elke Oetjen

Prüfungsausschuss, zweite/r Gutachter/in: Prof. Dr. Dr. Ralf Smeets

Inhaltsverzeichnis

1. Originalpublikation 2

2. Zusammenfassende Darstellung der Publikation 15

2.1 Einleitung.....15

2.2 Material und Methoden 16

2.3 Ergebnisse 19

2.4 Diskussion 21

2.5 Schlussfolgerung 25

2.6 Literaturverzeichnis.....25

3. Zusammenfassung 28

3.1 Zusammenfassung in deutscher Sprache 28

3.2 Zusammenfassung in englischer Sprache.....29

4. Erklärung des Eigenanteils 30

5. Danksagung 30

6. Lebenslauf.....31

6.1 Publikationen 32

7. Eidesstattliche Erklärung 34

1. Originalpublikation

135 (2022) 212740

Contents lists available at ScienceDirect

Biomaterials Advances

journal homepage: www.journals.elsevier.com/materials-science-and-engineering-c

Antibacterial properties of functionalized silk fibroin and sericin membranes for wound healing applications in oral and maxillofacial surgery

Sogand Schäfer [a,*], Ralf Smeets [a,b], Marius Köpf [c], Aleksander Drinic [c], Alexander Kopp [c], Nadja Kröger [d], Philip Hartjen [b], Alexandre Thomas Assaf [b], Farzaneh Aavani [a], Thomas Beikler [e], Ulrike Peters [e], Imke Fiedler [f], Björn Busse [f], Ewa K. Stürmer [g], Tobias Vollkommer [b], Martin Gosau [b], Sandra Fuest [a]

[a] Department of Oral and Maxillofacial Surgery, Division of Regenerative Orofacial Medicine, University Hospital Hamburg-Eppendorf, 20251 Hamburg, Germany
[b] Department of Oral and Maxillofacial Surgery, University Medical Center Hamburg-Eppendorf, 20251 Hamburg, Germany
[c] Fibrothelium GmbH, Aachen, Germany
[d] Department of Plastic, Reconstructive and Aesthetic Surgery, University Hospital of Cologne, 50937 Cologne, Germany
[e] Department of Periodontics, Preventive and Restorative Dentistry, University Medical Center Hamburg-Eppendorf, 20251 Hamburg, Germany
[f] Department of Osteology and Biomechanics, University Medical Center Hamburg-Eppendorf, 20251 Hamburg, Germany
[g] Department of Vascular Medicine, University Heart Center, Translational Wound Research, University Medical Center Hamburg-Eppendorf, 20251 Hamburg, Germany

ARTICLE INFO

Keywords:
Oral wound healing
Antibacterial wound dressing
Silk protein
Silver
Gentamicin
Electrospinning

ABSTRACT

Oral wounds are among the most troublesome injuries which easily affect the patients' quality of life. To date, the development of functional antibacterial dressings for oral wound healing remains a challenge. In this regard, we investigated antibacterial silk protein-based membranes for the application as wound dressings in oral and maxillofacial surgery. The present study includes five variants of casted membranes, i.e., *i*) membranes-silver nanoparticles (CM-Ag), *ii*) membranes-gentamicin (CM-G), *iii*) membranes-control (without functionalization) (CM-C), *iv*) membranes-silk sericin control (CM-SSC), and *v*) membranes-silk fibroin/silk sericin (CM-SF/SS), and three variants of nonwovens, i.e., *i*) silver nanoparticles (NW-Ag), *ii*) gentamicin (NW-G), *iii*) control (without functionalization) (NW-C). The surface structure of the samples was visualized with scanning electron microscopy. In addition, antibacterial testing was accomplished using agar diffusion assay, colony forming unit (CFU) analysis, and qrt-PCR. Following antibacterial assays, biocompatibility was evaluated by cell proliferation assay (XTT), cytotoxicity assay (LDH), and live-dead assay on L929 mouse fibroblasts. Findings indicated significantly lower bacterial colony growth and DNA counts for CM-Ag with a reduction of bacterial counts by 3log levels (99.9% reduction) in CFU and qrt-PCR assay compared to untreated control membranes (CM-C and CM-SSC) and membranes functionalized with gentamicin (CM-G and NW-G) ($p < 0.001$). Similarly, NW-G yielded significantly lower DNA and colony growth counts compared to NW-Ag and NW-C ($p < 0.001$). In conclusion, CM-Ag represented 1log level better antibacterial activity compared to NW-G, whereas NW-G showed better cytocompatibility for L929 cells. As data suggest, these two membranes have the potential of application in the field of bacteria-free oral wound healing. However, provided that loading strategy and cytocompatibility are adjusted according to the antibacterial agents' characteristic and fabrication technique of the membranes.

* Corresponding author.
E-mail addresses: sog.schaefer@uke.de (S. Schäfer), r.smeets@uke.de (R. Smeets), marius.koepf@fibrothelium.com (M. Köpf), aleksander.drinic@fibrothelium.com (A. Drinic), alexander.kopp@fibrothelium.com (A. Kopp), p.hartjen@uke.de (P. Hartjen), a.assaf@uke.de (A.T. Assaf), t.beikler@uke.de (T. Beikler), u.peters@uke.de (U. Peters), i.fiedler@uke.de (I. Fiedler), b.busse@uke.de (B. Busse), e.stuermer@uke.de (E.K. Stürmer), t.vollkommer@uke.de (T. Vollkommer), m.gosau@uke.de (M. Gosau), s.fuest@uke.de (S. Fuest).

https://doi.org/10.1016/j.bioadv.2022.212740
Received 9 November 2021; Received in revised form 13 February 2022; Accepted 25 February 2022
Available online 17 March 2022

1. Introduction

Wound healing is a complex, highly orchestrated process that includes well-defined overlapping phases known as hemostasis, inflammation, proliferation, and remodeling [1]. Both intra-oral and extra-oral wound healing require an interplay of signaling molecules (e.g., cytokines and growth factors) from blood cells and local tissue cells working in concert to heal the injured site towards a restored barrier function [2].

Depending on the lesion site, wound healing within the oral cavity can be categorized as periodontal healing, dental implant interfaces healing, dental pulp healing, and bone healing [3]. The saliva-filled environment of the oral cavity provides various proteinaceous substances, such as growth factors (epidermal growth factor, vascular endothelial growth factor, and fibroblast growth factors) and histatins, accelerating the wound healing process. Oral wounds have an increased healing potential compared to skin wounds [4]. This is attributed to faster initiation of the inflammatory phase, lower levels of immune mediators, more bone marrow-derived cells, fast re-epithelialization, and rapid fibroblast proliferation [5]. Most importantly, due to favorable anatomical relations, the oral cavity has excellent access to steady blood flow.

Up to now, several approaches have been introduced to heal oral wounds [5–7]. The state-of-the-art in oral and maxillofacial surgery is the utilization of autologous mucocutaneous flaps for or allogenic/xenogeneic grafts, e.g., acellular dermal matrices (ADM), depending on the extent of the soft tissue defect. However, flaps are associated with donor site morbidity and unsatisfactory cosmetic outcomes, whereas ADMs have shown to induce inflammatory reactions, antigenicity, and, additionally, are limited in resources [8,9]. Generally, the healing process of wounds can be accelerated using biomedical engineered structures such as hydrocolloids, films, gauze, hydrogels, foams, and hydrofibers [10]. One of the best-known approaches for oral wound healing is the application of polymer-based membranes [11]. So far, various natural biomaterials have been introduced to promote the oral wound healing process, including collagen [12], alginates [13,14], chitosan [15], and gelatin [16]. Other natural biomaterials such as the silk proteins silk fibroin (SF) and silk sericin (SS) have gained increasing attention due to their remarkable mechanical properties, superior biocompatibility, oxygen, and water vapor permeability, controllable proteolytic degradability, and minimal immunogenicity [17]. Composed of fibroin (70–80%) and sericin (20–30%), the proteins are extracted from the cocoons of the silkworm *Bombyx mori* (*B. mori*) through different well described methods [18]. Silk proteins have shown to complement each phase of the wound healing process, hence, can be broadly used as wound dressings for acute and chronic wound healing [19]. SF interacts with blood components, e.g., platelets and fibrin, initiating the clotting cascade [20]. Additionally, SF and SS materials accelerate the initial inflammatory response, however, they do not prolong this phase. According to in vitro and in vivo studies, SF can significantly decrease the leucocyte count and overall inflammation, which is an advantageous feature in this process [21,22]. Moreover, SF and SS were able to accelerate the proliferation of a variety of human cells in vitro and in vivo, leading to defect site coverage with native tissue and neovascularization [19,20,23]. According to the applicational demand, silk protein-based substances can be manufactured into various forms (e.g., fibers, films, gels, and three-dimensional scaffolds). As an example, the successful utilization of silk proteins as substrates for electrospinning resulted in the fabrication of mechanically advanced membranes for the wound healing process [24]. To further promote biological host responses, prior to electrospinning, different signaling molecules such as growth factors and polypeptides can be incorporated into the silk protein solution [24–26].

Despite the recent progress in oral wound healing, there are some challenging points in the fabrication of membranes for oral wound healing. The oral mucosa is a warm and moist environment which creates an excellent microenvironment for the habitation of bacteria such as *Streptococcus mutans*, *Actinomyces naeslundii*, *Fusobacterium nucleatum* and *Porphyromonas gingivalis*, decreasing the efficacy of the wound healing process. To avoid bacterial growth at the wound site, different antibacterial agents can be incorporated into the wound dressing. Metallic nanoparticles such as silver, magnesium, zinc, or copper have been successfully used to fabricate skin wound dressings with antibacterial activity [27,28]. Silver nanoparticles (AgNPs) in particular are known to contain bacterial growth and display anti-inflammatory properties [29,30]. However, establishing a balance between the antibacterial activity and cytotoxicity potential of AgNPs should be precisely considered. In addition to metal ions, some antibiotics such as penicillins, aminoglycosides, or glycopeptides have been used to modify wound dressings [31,32]. Gentamicin, an aminoglycoside antibiotic, is broadly applied to treat bacterial skin and soft tissue infections [33–35]. A recent investigation by Zhou et al., proposed the idea of combining favorable effects of the two most common antibacterial functional agents AgNPs and gentamicin with an SF/Chitosan dental implant coating. With this approach, the authors could produce antibacterial implant coatings that significantly inhibited bacterial growth, adhesion, and biofilm formation with improved support of preosteoblastic MC3T3 cells and osteoblast growth [36]. Combining the excellent properties of silk materials with antibacterial agents presents an advanced approach in this matter.

In spite of experimental efforts in developing a functional wound dressing for the skin, the application of antibacterial loaded silk protein membranes for oral wound healing has not been evaluated so far. Hence, in this in vitro study, we investigated advanced antibacterial silk protein membranes. Using casting and electrospinning techniques, casted membranes (CM) and nonwovens (NW) had been functionalized with AgNPs and gentamicin prior to our investigation. The aim of this study was the evaluation of antibacterial membranes for wound healing applications in oral and maxillofacial surgery.

2. Materials and methods

2.1. Manufacture of SS/SF membranes

For the manufacture of the fibroin membranes, *B. mori* silk cocoons were used for protein extraction. The procedure was performed according to the PureSilk® technology of the company Fibrothelium GmbH. Briefly, fibroin was separated from sericin by degumming it in a hot alkali solution before dissolving it in a solvent system based on Ajisawa's reagent. The dissolved fibroin was dialyzed against VE water for 48 h. The initial concentration of the resulting fibroin solution was 3 wt%. The solution was then stored at 4 °C.

For the SS substrate, an SS solution was obtained by degumming *B. mori* silk cocoons with 8 M urea solution (1:44.414). The urea solution was heated to 80 °C with the cocons which were degummed for 3 h while being stirred with a magnetic stirrer. After 3 h the cocoons were transferred into a sieve and rinsed with deionized water. The cocoons are then soaked 3 times for 3 min to rinse out residual degumming solution. The SS-urea solution was transferred into dialysis membranes (MWCO 3.5 kDa) and dialyzed against water for 48 h while exchanging the water two times a day. Two structural types of materials based on SS were manufactured: casted membranes (CM) and nonwovens (NW).

For functionalization, three variations of SF-nonwovens (gentamicin, silver, and untreated fibroin controls) and five variations of SS and/or SF-membranes (gentamicin, silver, untreated fibroin controls, SF/SS, and untreated sericin controls) were manufactured (Table 1). First, the SF or SS solution was casted on a PTFE mold. After drying for 24 h at 21 °C under a laminar hood, the final fibroin membrane had a thickness of approximately 0.1–0.2 mm. The thickness was determined by a digital micrometer (Micromar 40 ER, Mahr GmbH, Germany).

For functionalization, the fibroin solution was priorly mixed with gentamicin or silver nitrate (AgNO3). For the $AgNO_3$-functionalized membranes, the mixed solution was UV irradiated for 1 h before casting. SF NWs were electrospun and directly afterwards post-treated in an

Table 1
Functionalization and sample size of SF and SS membranes.

Material (CM/NW)	Sample size/material (n)	Pre-treatment	Fibroin (3 w%)	Sericin (3 w%)	Gentamicin (10 mg/mL)	$AgNO_3$	Post-treatment	Abbreviation
NW	10	–	20 mL	–	–	–	Ethanol (70 v%)	NW-C
NW	10	–	20 mL	–	10 mL	–	Ethanol (70 v%)	NW-G
NW	10	UV irradiation	20 mL	–	–	0.1 g	Ethanol (70 v%)	NW-Ag
CM	10	–	20 mL	–	–	–	Ethanol (70 v%)	CM-SFC
CM	10	–	20 mL	–	10 mL	–	Ethanol (70 v%)	CM-G
CM	10	UV irradiation	20 mL	–	–	0.1 g	Ethanol (70 v%)	CM-Ag
CM	10	–	10 mL	10 mL	–	–	Ethanol (70 v%)	CM-SF/SS
CM	10	–	–	20 ml	–	–	Ethanol (70 v%)	CM-SSC

ethanol bath (70 v%) for 1 h to obtain insolubility. In a next step, the SF NWs were immersed in $AgNO_3$ solution or gentamicin for around 60 min. The $AgNO_3$ treated NWs samples were also UV irradiated.

Flexible SS films were obtained by adding glycerol to the SS solution. In this case the glycerol added, amounted to 30 wt% of the total mass of SS in a defined volume. The solution was then stirred for 5 min to ensure homogeneous mixture of glycerol. Subsequently the SS-glycerol solution was casted onto a PTFE mold and left to dry under a laminar hood at ambient temperature for 48 h. Finally, the dried films were treated with 70 v% ethanol before peeling them off the PTFE sheet. The films were then stored in press-seal bags at ambient temperature until further use.

Finally, all materials were stored in 70 v% ethanol at 4 °C. An overview of functionalization and sample size is given in Table 1.

2.2. Scanning electron microscopy

The surface morphology of the samples was analyzed utilizing scanning electron microscopy (SEM) (Crossbeam 340, Zeiss, Oberkochen, Germany). Prior to imaging, samples were dried under a laminar floor hood for 7 days. A clear cut was performed through the samples' midline with a scalpel for cross-sectional imaging. Samples were then affixed on a sample holder, and subsequently gold-sputtered to provide electron stability (sputter coater S150B, Edwards, London, UK). Imaging was performed in secondary electron (SE) mode at an acceleration voltage of 5 kV, working distance of 5 mm, and at magnifications ranging from 500× to 10.000×.

2.3. Cytocompatibility analysis

Cytocompatibility assessment was proceeded according to our former work [37].

2.3.1. Reference materials (toxic and non-toxic controls)

A polyurethane film containing 0.1% zinc diethyldithiocarbamate (ZDEC) (Hatano Research Institute, Kanagawa, Japan) was used as toxic control substance for all cytocompatibility assays. For the indirect assays, medium that was incubated in the absence of specimens was used as a non-toxic control. For the live-dead staining assay, tissue culture coverslips (TCC) (Sarstedt, Nümbrecht, Germany, Cat. No. 83.1840.002) were used as a non-toxic control material.

2.3.2. Cell culture

L929 mouse fibroblasts were obtained from the European Collection of Cell Culture, ECACC (Salisbury, UK). Cells were cultured in MEM supplemented with 10% fetal bovine serum, glutamine to final concentration of 4 mM and penicillin/streptomycin (100 U/mL each) (all from Life Technologies, Carlsbad, USA), in the following referred to as cell culture medium, at 37 °C, 5% CO_2 and 95% humidity (cell culture conditions). Cells were passaged when they reached approximately 80% confluency.

2.3.3. Extraction

The materials were washed three times for 30 min in 1 mL cell culture medium to remove the storage solution (70 v% ethanol) and to saturate the samples with medium. The materials were then extracted at a ratio of 3 cm^2/mL of cell culture medium for 72 h at 37 °C, 5% CO_2, and 95% humidity (cell culture conditions).

2.3.4. Indirect assay procedure

96-Well plates (Sarstedt, Nümbrecht, Germany) were seeded with 1 × 10^4 cells/well in 100 µL cell culture medium and incubated under cell culture conditions for 24 h. Thereafter, cell culture medium was discarded and 100 µL of extract was added to each well. Cells were further incubated for 24 h and then subjected to the XTT-assay, while the supernatants were subjected to the LDH-assay.

2.3.5. Viability assay

Cells incubated with the extracts were subjected to an XTT-assay. The "Cell Proliferation Kit II" (XTT) (Roche Diagnostics, Mannheim, Germany) was used according to the manufacturers' instructions. Briefly, the electron-coupling reagent was mixed with XTT labeling reagent (1:50 dilution) and 50 µL of the mixture was added to the cells. After 4 h of incubation under cell culture conditions, substrate conversion was quantified by measuring the absorbance of 100 µL aliquots in a new 96-well plate using a scanning multi-well spectrophotometer (Microplate Reader, Bio-Rad Laboratories, Inc., CA, USA) with filters for 450 nm and 650 nm (reference wavelength).

2.3.6. Cytotoxicity assay

Cytotoxicity was determined using a "LDH-Cytotoxicity Assay Kit II" (BioVision, Milpitas, CA, USA) according to the manufacturers' instructions. Briefly, 10 µL of the cell supernatants were incubated with 100 µL LDH reaction mix for 30 min at room temperature. After addition of stopping solution, absorbances were measured using a scanning multi-well spectrophotometer (Microplate Reader, Bio-Rad Laboratories, Inc., CA, USA) with filters for 450 nm and 650 nm (reference wavelength).

2.3.7. Live-dead staining assay

In order to perform live-dead cell staining on the surfaces of the membrane specimens, 60 µL per mL medium propidium iodide (PI) stock solution (50 µg/mL in PBS) and 500 µL per mL medium fresh fluorescein diacetate (FDA) working solution (20 µg/mL in PBS from 5 mg/mL FDA in acetone stock solution) were added to each well (12 well plate). After a brief incubation for 3 min at room temperature, specimens were rinsed in prewarmed PBS and immediately examined with an upright fluorescence microscope (Nikon ECLIPSE Ti-S/L100, Nikon GmbH, Düsseldorf, Germany) equipped with a filter for parallel detection of red and green fluorescence.

2.3.8. Data evaluation

The mean absorbance of the blank controls without cells was subtracted from the mean absorbances and data was normalized to the negative control.

2.4. Antibacterial activity

An overview of the antibacterial testing strategy is illustrated in

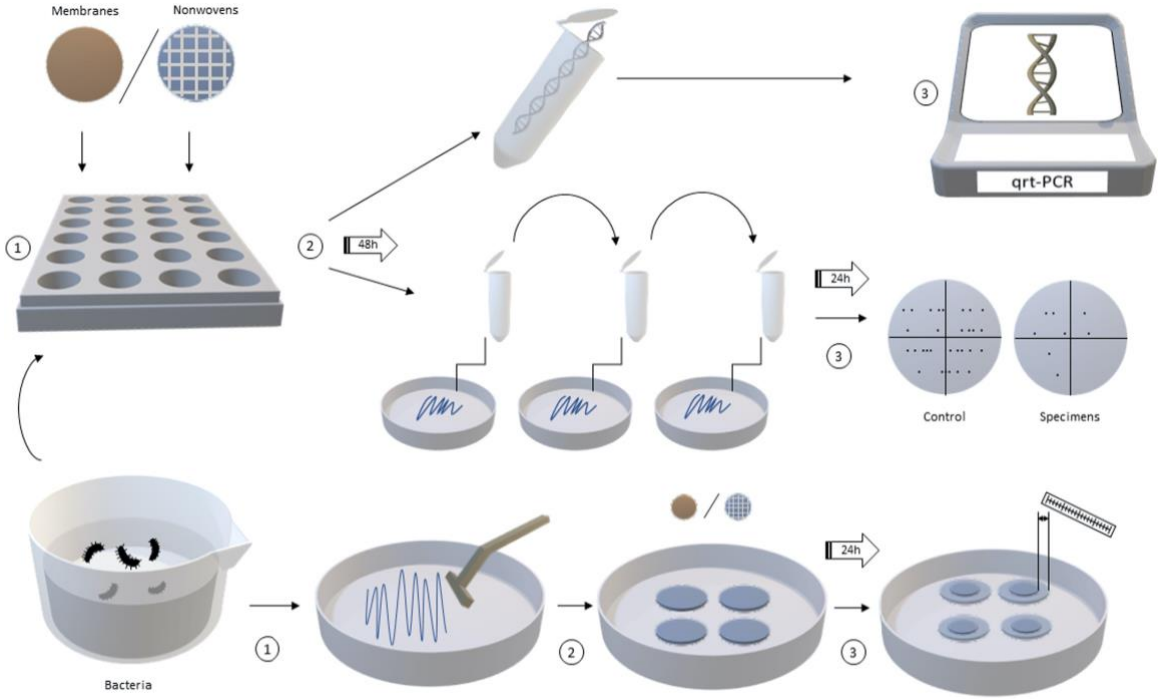

Fig. 1. Antibacterial testing strategy. Two structural forms of SF and SS materials, i.e., CMs and NWs were manufactured. 1. Materials were either placed in 24-well plates preincubated with bacterial mixed culture solution, or the materials were plated on blood agar plates previously incubated with bacterial mixed culture solution. 2. For the first test, an incubation time of 48 h, for the second test, an incubation time of 24 h was chosen. 3. Antibacterial activity was assessed through qrt-PCR, CFU analysis, and zone of inhibition (ZOI).

Fig. 1.

2.4.1. Antibacterial activity analysis of total and viable bacterial count

All specimens were stored in 70 v% ethanol (EtOH), consequently, specimens were considered sterile. A sample size of $n = 10$ specimens per structure (CM or NW) and functionalization, i. e., untreated SS/SF controls (CM-C, CM-SSC, NW-C), loaded with silver ions (CM-Ag, NW-Ag), and loaded with gentamicin (CM-G, NW-G), was incubated for 24 h in artificial saliva, which was comprised of a-amylase 1 mg/mL, mucin 0.85 mg/mL, and bovine serum albumin (BSA) 0.4 mg/mL.

Cultivation of bacterial strains and following treatment of the specimens was performed in anaerobic conditions at 37 °C in Whitley A35 Workstation (Whitley A35 Workstation Don Whitley Scientific, Bingley, United Kingdom).

In order to create a liquid bacterial mixed culture, anaerobic stains of early colonizing *Streptococcus mutans* (*Streptococcus mutans*, DSM 20523, German Collection of Microorganisms and Cell Cultures GmbH, Leibnitz, Germany), moderate colonizing *Actinomyces naeslundii* (*Actinomyces naeslundii*, DSM 17233, German Collection of Microorganisms and Cell Cultures GmbH, Leibnitz, Germany), *Fusobacterium nucleatum* (*Fusobacterium nucleatum*, DSM 15643, German Collection of Microorganisms and Cell Cultures GmbH, Leibnitz, Germany), and late colonizing *Porphyromonas gingivalis* (*Porphyromonas gingivalis*, DSM 20709, German Collection of Microorganisms and Cell Cultures GmbH, Leibnitz, Germany) were separately cultivated on blood agar plates. Subsequently, each strain was transferred into bacterial culture medium (CDC Anaerobe 5% Sheep Blood), and after sufficient observable growth (usually after 2–5 days), 1 mL of each strain was mixed into 20 mL CDC medium. Mixed bacterial culture optical density (OD) was 0.1.

Test membranes were placed onto 24-well plates. Each well was previously filled with 1.5 mL mixed bacterial culture suspension. After an incubation time of 48 h, membranes were separately moved into sterile 1.5 mL Eppendorf tubes, vortexed, and a total of 100 μL sample was taken from each Eppendorf tube for total and viable bacterial count analysis. Viable bacterial count was tested by inoculating blood agar plates with 50 μL sample in dilutions of 1:100, 1:1000, 1:10.000 and the Colony Forming Unit (CFU) was measured. Total bacterial DNA count was measured through Polymerase Chain Reaction (PCR) by processing 50 μL sample with DNA Isolation Kit (innuPREP DNA Isolation Kit, Analytik Jena AG, Jena, Germany) and quantifying the DNA amount with qrt-PCR (quantitative Real-Time-PCR, CFX96 Touch Real-Time PCR Detection System, Bio-Rad Laboratories, Berkeley, California, USA) utilizing a universal eubacterial 16S-rRNA primer (HDA1-GACTCCTACGGGAGGCAGCAGT, E1115RAGGGTTGCGCTCGTTGCGGG) and specific Primers (Table 2).

2.4.2. Direct antibacterial activity analysis

Direct antibacterial activity was evaluated in an agar diffusion test. For this purpose, five blood agar plates for each material and functionalization were inoculated with either mixed bacterial culture solution or isolated liquid culture of the bacterial strains, respectively. Two samples of each material and functionalization were directly taken from storage tubes, briefly drained, and placed on the agar plates. After an incubation time of 24 h, respective inhibition zones were measured with a micrometer screw gauge.

2.5. Data evaluation

For the cytocompatibility assays, the mean absorbance of the blank controls without cells was subtracted from the mean absorbances and

Table 2
Specific primer sequences for qrt-PCR and references of their applicability according to our former work [38].

Organism	Primer	Primer sequence	Reference of primer applicability
Porphyromonas gingivalis	CA-PG-F/R	AGGCAGCTTGCCATACTGCG ACTGTTAGCAACTACCGATGT	Carrouel F. et al., 2016 [39].
Streptococcus mutans	MKD-FV/RV	GGCACCACAACATTGGGAAGCTCAG GGAATGGCCGCTAAGTCAACAGG	Hoshino T. et al., 2004 [40].
Actinomyces species	ACT-174-F ACT-281-R	GGTCTCTGGGCCGTTACTGA GRCCCCCCACACCTAGTG	Ellerbrock B., 2010 [UKD].
Fusobacterium nucleatum	CA-FN-F/R	AGAGTTTGATCCTGGCTCAG GTCATCGTGCACACAGAATTGCTG	Carrouel F. et al., 2016 [39].

data was normalized to the negative control. Statistical analysis of the antibacterial tests was conducted using SAS 7.4 (SAS Institute Inc., Cary, North Carolina, USA). Mean bacterial DNA counts from qrt-PCR measurement and CFU analysis values were evaluated. For the qrt-PCR and CFU analysis results an exponential-linear model was chosen. *P*-values < 0.05 were considered statistically significant.

3. Results

3.1. Structural analysis

Fibroin nonwovens comprised a highly porous structure, created through highly intertwining fibers compared to the smooth surface of the SF and SS casted membranes. Cross-sectional imaging shows upheld continuity of fiber connections within the whole thickness of the NWs. Some CMs present a layered appearance in cross-section, presumably cutting artifacts.

The CM-C and CM-SSC present a rough topography distinguishable from gentamicin and silver CMs. Conversely, NW-C appear to have a smooth fiber surface texture, whereas the NW-Ag appear to present a more uneven fiber surface texture within 10,000× magnification imaging (Fig. 2).

3.2. Cytocompatibility

With the exception of the silver loaded materials (CM-Ag, NW-Ag), all membranes had sufficient cytocompatibility with viability values >70% of the negative control in the indirect assay which indicates the non-toxic range as defined in in current, international standards (DIN EN ISO 10993-5:2009, German Institute for Standardization, Berlin, Germany) (Fig. 3). The viability was similar (range 91%–108% of the negative control) for all materials except for the silver loaded specimens (4% of the negative control) ($p < 0.001$). Cytotoxicity values for all specimens were consistent – showing a similar range as the negative control (cells incubated with cell culture medium) for all materials except for the silver specimens, indicating low cytotoxicity (Fig. 4). Notably, silver specimens yielded negative values in the LDH assay, thus, silver ions were suspected to interfere with the assay. Therefore, assay interference testing was conducted. For this purpose, the LDH-assay was repeated with the material extracts omitting cells, resulting in negative extinction values for the silver loaded materials (data not shown). Additionally, the silver loaded materials were extracted together with the toxic control (RM-A) and the LDH-assay was repeated again, resulting in an apparent RM-A toxicity that was decreased by the

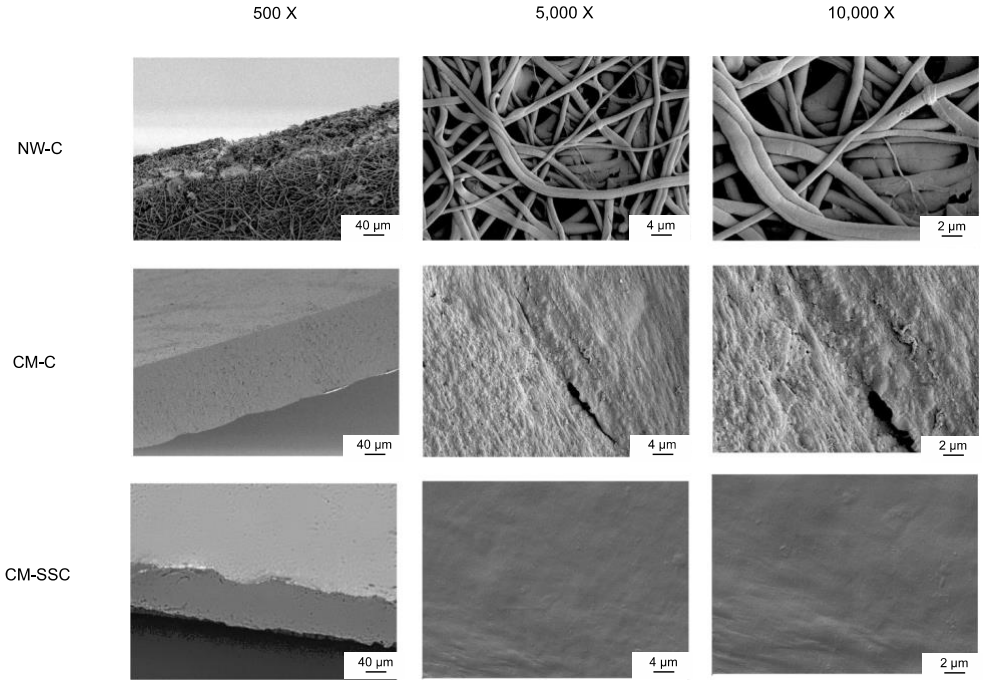

Fig. 2. SEM imaging of SF and SS materials with three magnifications (500×, 5000×, and 10,000×). Depicted are control CMs and NWs. Imaging of the other specimens (NW-G, NW-Ag, CM-G, CM-Ag, CM-SF-SS) can be found in the Supplementary data.

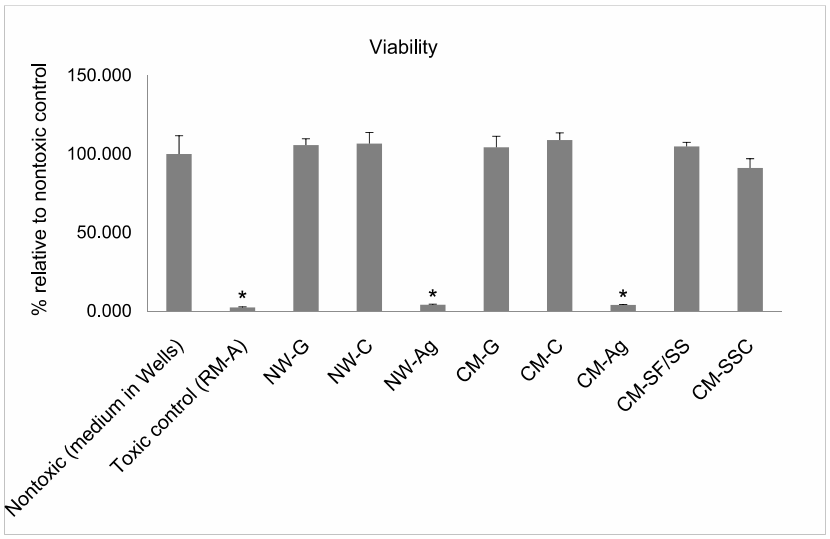

Fig. 3. Viability of L929 fibroblasts after extract application of SF and SS materials with/without active agents: gentamicin, silver, combined SF/SS, and control casted membranes (CM-G, CM-Ag, CM-SF/SS, CM-C, CM-SSC) and gentamicin, silver, and control NWs (NW-G, NW-Ag, NW-C); $n = 10$/group. Abbreviations according to Table 1. Data are expressed as MV + STD; *$p > 0.05$ compared to nontoxic control.

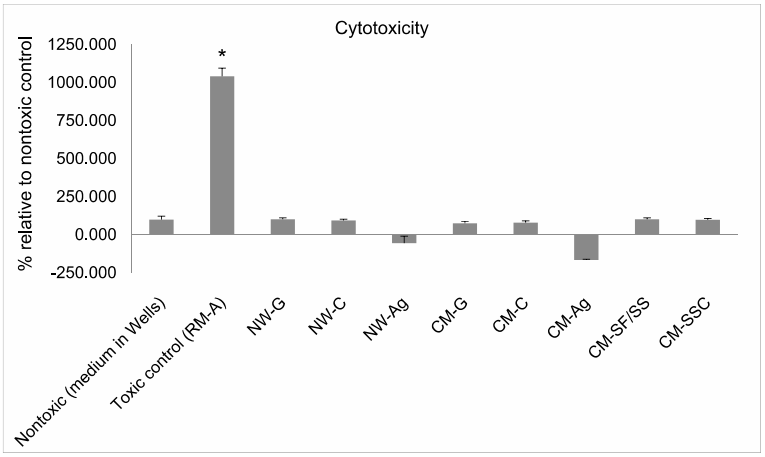

Fig. 4. Cytotoxicity assay with L929 fibroblasts after extract application of SF and SS materials with/without active agents: gentamicin, silver, combined SF/SS, and control casted membranes (CM-G, CM-Ag, CM-SF/SS, CM-C, CM-SSC) and gentamicin, silver, and control nonwovens (NW-G, NW-Ag, NW-C); $n = 10$/group. Abbreviations according to Table 1. Data are expressed as MV + STD; *p > 0.05 compared to nontoxic control.

same magnitude as the materials were suspected to interfere with the assay (not shown), strongly suggesting assay interference by the silver ions and thus false negative cytotoxicity values for the silver loaded materials.

Live-dead staining revealed large numbers of green fluorescein diacetate (FDA) positive vital cells with only sporadic red propidium iodide (PI) positive dead cells visible on all materials except for the silver loaded specimens which were covered with much fewer cells indicating weak attachment and/or cytotoxicity (Fig. 5). On all materials, with the exception of the silver loaded specimens, at least some spindle shaped cells, with fibroblast characteristic morphology were detected. The cells on the silver loaded specimens were rounded, suggesting weak attachment or cytotoxicity. The assessment of NW-Ag and NW-C was limited because these materials underwent a deformation process upon hydration after contact with the cell culture suspension. Overall, these results indicate that all materials except for the silver loaded specimens are cytocompatible.

3.3. Antibacterial activity

3.3.1. Viable bacterial count

CFU analysis showed significantly lowest colony growth for CM-Ag ($p < 0.0001$) compared to all other groups followed by CM-G and NW-G ($p < 0.02$) (Fig. 6). CM-Ag decreased bacterial DNA count by 3 log-reductions compared to the positive control (bacterial mixed culture solution), implying a reduction of 99.9%. No significant difference could

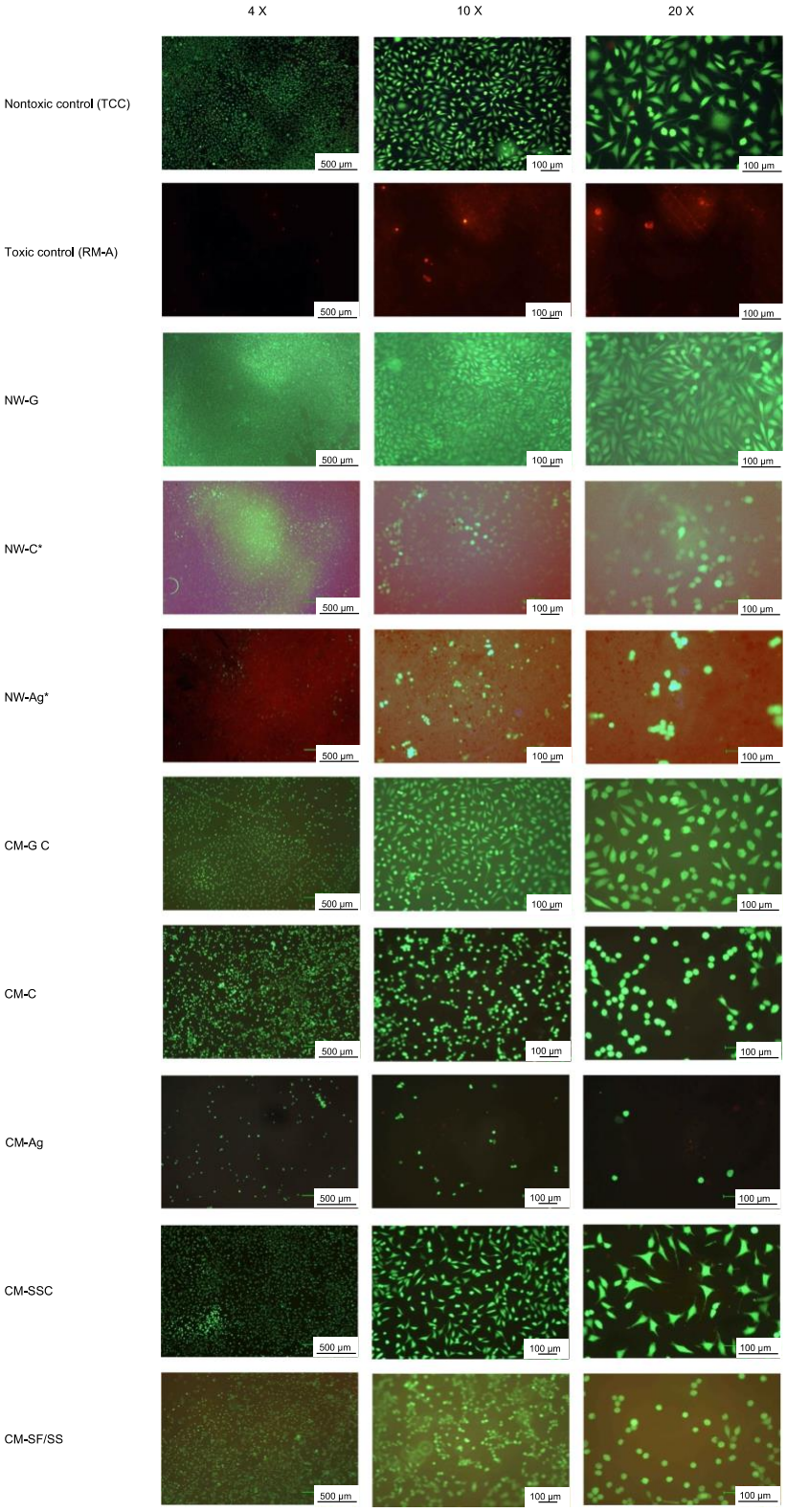

Fig. 5. Live-dead staining assay with L929 fibroblasts seeded on membranes with/without active agents: gentamicin, silver, combined fibroin-sericin, and control casted membranes (CM-G, CM-Ag, CM-SF/SS, CM-C, CM-SSC) and gentamicin, silver, and control nonwovens (NW-G, NW-Ag, NW-C); $n = 10$/group. Abbreviations according to Table 1.
*Specimens underwent a deformation process upon hydration after contact with the cell culture suspension impeding accurate imaging.

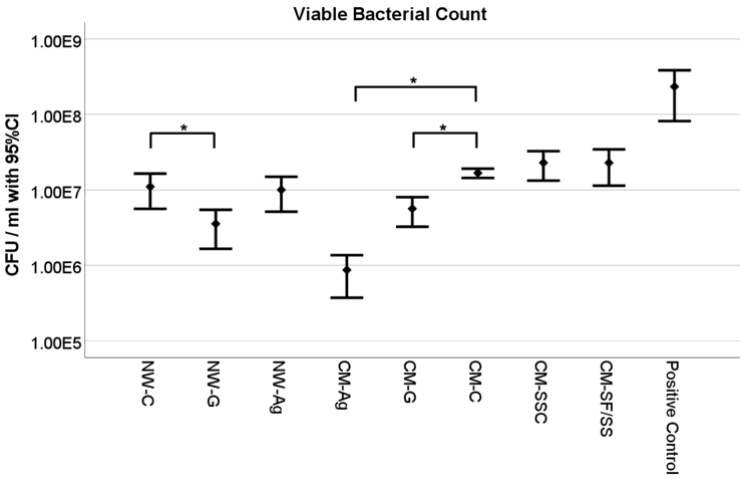

Fig. 6. Colony Forming Unit/mL of SF and SS materials after 48 h of specimen incubation on plated mixed bacterial culture solution. Mean values with 95% confidence interval are given in logarithmic scale unit. Results indicate viable bacterial count. n = 10/group. All groups were compared to each other (Section 3.3.1). For clarity, the parentheses indicate the results for the loaded nonwoven materials compared to the nonloaded nonwoven control (NW-C) and the results for the loaded membrane materials compared to the nonloaded casted membrane control (CM-C), $^*p > 0.05$.

be detected between CM-G and NW-G. NW-Ag showed similar CFU values as the control NW-C ($p = 0.7$). CM-SF/SS and the controls CM-SSC and CM-C showed CFU-values of similar range with $p = 0.9$ and $p = 0.6$, respectively. All tested materials had significantly lower CFU values compared to the positive control (bacterial mixed culture solution) ($p < 0.0001$). In a sum, bacterial viability was inhibited in the following order from best to least effectivity: CM-Ag, NW-G, CM-G, NW-Ag, NW-C, CM-C, CM-SSC, and CM-SF/SS.

3.3.2. Total bacterial count

As presented in Fig. 7, all tested membranes had significantly lower bacterial DNA counts compared to the positive control ($p < 0.0001$) with the lowest DNA count for CM-Ag among all comparison groups ($p < 0.0001$). CM-Ag decreased bacterial DNA count by 3 log-reductions compared to the positive control implying a reduction of 99.9%. Consistent with CFU results, no statistical difference was found between the CMs-G and NW-G ($p = 0.1$). Notably different to CFU results, NW-Ag had significantly lower bacterial DNA copies compared to the control NW-C ($p < 0.005$), indicating a containment of total bacterial counts. According to the measurement with specific primers (data not shown), positive deflections of the PCR analysis in all membranes presented *S. mutans* and *F. nucleatum* as most prevalent bacterial colonies followed by small amounts of *P. gingivalis* and *A. neaslundii*. No significant intergroup differences were present. In a sum, total bacterial count was inhibited from best to least in the following order: CM-Ag, NW-G, CM-G, NW-Ag, NW-C, CM-C, CM-SSC, and CM-SF/SS.

3.3.3. Direct antibacterial activity

For both material types, casted membranes and nonwovens, the largest inhibition zone of 7–8 mm was found for gentamicin loaded samples (CM-G, NW-G) and the second largest inhibition zone of 2–3 mm was found for silver loaded samples (CM-Ag, NW-Ag). No inhibition zone was detected for the untreated controls (CM-C, CM-SSC, NW-C) (Fig. 8). Accordingly, the combined SF/SS membranes yielded no zone of inhibition, either. With the specialized agar diffusion test it could be shown that gentamicin loaded membranes show an antibacterial activity against strains of *A. neaslundii*, *F. nucleatum*, and *S. mutans*, in descending order, whereas silver loaded membranes present

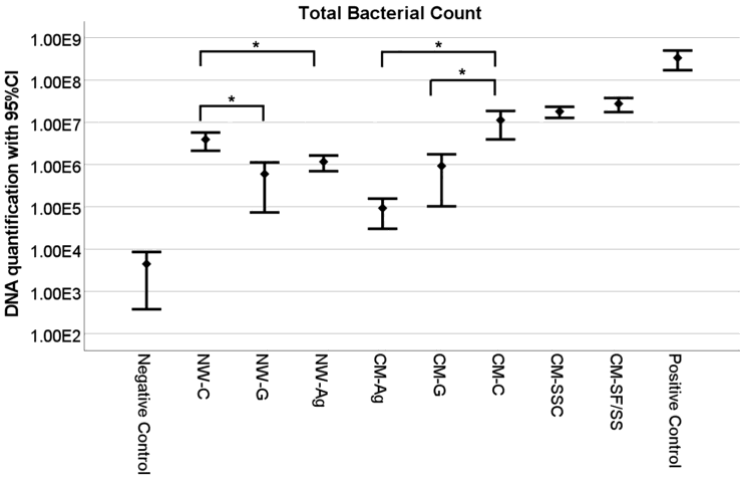

Fig. 7. Quantification of mean bacterial DNA copies measured by qrt-PCR (Universal Poly-Primer results) after 48 h for SF and SS membranes. Mean values with 95% confidence interval are given in logarithmic scale unit. qrt-PCR results indicate total bacterial count. $n = 10$/group. All groups were compared to each other (Section 3.3.2). For clarity, the parentheses indicate the results for the loaded nonwoven materials compared to the nonloaded nonwoven control (NW-C) and the results for the loaded membrane materials compared to the nonloaded casted membrane control (CM-C), $^*p > 0.05$.

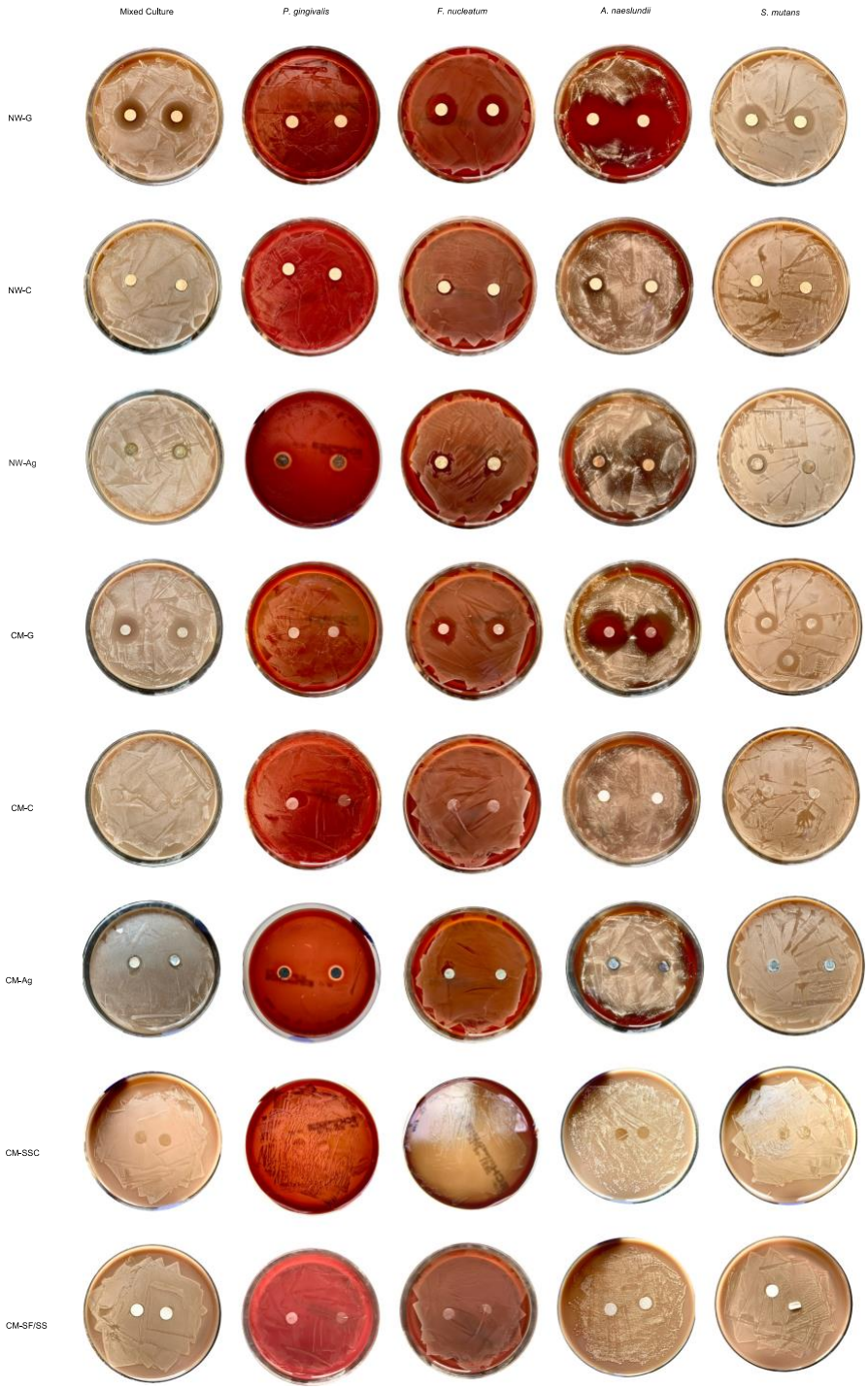

Fig. 8. Direct antibacterial activity assessment of SF and SS materials with agar diffusion test on bacterial mixed culture solution and selective bacterial strain solutions, respective zone of inhibition was measured with a micrometer after 24 h of incubation. n = 10/group.

antibacterial activity against *P. gingivalis* and *A. neaslundii* only. The CM-SF/SS and control membranes presented no inhibition zone, however, all test specimens prevented bacterial growth beneath the placement site.

In sum, the most pronounced direct antibacterial activity within all tested materials can be assigned to gentamicin loaded membranes followed by silver membranes.

4. Discussion

The healing of oral and maxillofacial wounds is a particularly challenging research area in the field of nanobiotechnology and tissue engineering. This importance can be attributed to specific features of the oral cavity [3], where a balance between pathogenic and commensal bacteria is needed to establish a state of homeostasis within the oral cavity [41]. Thus, a slight imbalance can lead to the development of caries, periodontitis, mucositis, and, eventually, to soft and hard tissue damage [42]. To avoid such impairments, the development of biomaterials able to inhibit the growth of pathogenic bacteria and, concurrently, to promote the wound healing process is needed [43]. In this context, the aim of this in vitro study was the characterization of antibacterial silk protein-based CMs and NWs for wound healing applications in oral and maxillofacial surgery and the implementation as wound coverages in plastic and reconstructive surgery.

The selection of a versatile biocompatible material is one of the most challenging points in the field of wound healing in oral and maxillofacial surgery due to the delicacy and sensitivity of the targeted tissue. So far, collagen, a promising biopolymer, has been broadly used to fabricate biodegradable wound dressing materials for surgical defects of the oral mucosa. For instance, in a clinical study by Rastogi et al., purified bovine collagen was employed to fabricate membranes for the treatment of secondary defects of the oral mucosa in 60 adult patients [44]. These defects appeared after excision of premalignant lesions and other conditions, such as incisional biopsy wounds. After using these membranes, the desirable levels of hemostasis, epithelialization and granulation were observed at the lesion sites. Accordingly, it was suggested that collagen membranes can be biologically acceptable wound graft materials for the oral mucosa. In another similar clinical studies, Omura et al., manufactured a bilayer membrane composed of silicone as the outer side, and dehydro-thermally cross-linked composites of collagen sponge as inner side [45]. Then, they put these membranes on oral mucosal defects in five patients after the surgery for cancers including Pleomorphic adenoma, Squamous cell carcinoma and Leukoplakia. It was observed that after 4–5 weeks, the collagen membrane formed a connective tissue after the migration of epithelial cells that made the repair effective. However, apart from the benefits, applying collagen as the membrane for wound healing has some challenging points. For instance, due to extraction from natural sources, collagen may cause immunogenicity. In addition, it may be subjected to gradual destruction during collagenolysis and inflammatory reactions. This procedure leads to weakening of the collagen membrane and mechanical instability of the graft within the oral cavity which may cause inconveniencies for the patients. Therefore, some research groups preferred to use other substitutes such as phospholipid [46], chitosan [47], polylactic galactic acid/polycaprolactone (PLGA/PCL) [48], carboxyvinyl polymer [49], hydrochloride gel [50], fibrin [51] etc., for the fabrication of membranes intended to heal mucosal wounds in the oral cavity. Focusing on the unique properties of silk proteins, we investigated the applicability of SF and SS membranes for intra-oral wound healing and thoroughly investigated nonwovens as well as casted membranes with respect to their antibacterial properties. It is well proved that silk nano-fibrous structures represent superior attachment and proliferation of fibroblast and keratinocytes, thus, improving the healing process of wounds in mucosal tissues [52,53]. Correspondingly, Tang et al. investigated the wound healing ability of electrospun SF matrices on buccal mucosa in rat models [54]. They concluded SF electrospun matrices promote the healing process and improve an anti-inflammatory host response. Also, they suggested that their developed mates can be a good substitute for ADMs. Similar results were reported in an in vivo study by Ge et al. in which SF scaffolds were applied on buccal defects in rat models [55]. For the application in wound healing, a vicinity of cells of the damaged tissue needs to be addressed and adequate biocompatibility is inevitable. In several studies, the good biocompatibility of silk-based scaffolds has been investigated [56,57]. In this experiment, we performed XTT, LDH, and *live/dead staining* assay on L929 mouse fibroblasts. The results of the XTT and LDH assay demonstrate sufficient cytocompatibility for all gentamicin-modified membranes. These findings illustrated a safe, tolerable usage dose of 10 mg/mL gentamicin for L929 mouse fibroblasts. Similar outcomes were obtained by Stevanović and colleagues [58], demonstrating well tolerable concentrations of gentamicin below 50 mg/mL on L929 cells. In contrast to this, CMs and NWs containing AgNPs decreased the L929 cell line in XTT assay and demonstrated cytotoxicity in LDH assay as well as in live/dead assay. According to our observations, we concluded that high concentrations of AgNPs corresponded with higher cytotoxicity, which was the case at 100 mg/L in this study. It is suggested that the cell toxicity of AgNPs and silver ions results from triggering oxidative stress in cells [59]. Indeed, AgNPs generate a high level of intracellular reactive oxygen species (ROS) and negatively affect the activity of antioxidant enzymes. These events disrupt normal cell function and cause disintegration of the cell membrane inducing apoptotic signaling pathways in cells [60]. Moreover, AgNPs can bind to functional groups of cell proteins and subsequently, trigger physicochemical interactions within cells [61]. Most studies report a safe, non-cytotoxic application of AgNPs at concentrations of $\leq$25 mg/L [62,63]. AgNP cytotoxicity might vary with the size of the nanoparticles in an inversely proportional fashion, yielding decreased cytotoxicity with bigger particle size due to lower surface area to volume ratio [64–67].

In this investigation, the main goal for the fabricated membranes with AgNPs and gentamicin was to induce antibacterial properties in these structures. The use of silver as an antibacterial substance in regenerative medicine has been investigated for decades [68,69]. The mode of antibacterial action of silver was found to be through membrane permeability disruption which results in the loss of intracellular K^+ ions, ATP and phospholipids. In addition, AgNPs cause oxidative damage by producing reactive oxygen species (ROS) and subsequently leaking intracellular metabolites through permeabilized membranes [70]. On the other hand, the aminoglycoside antibiotic, gentamicin, has a mechanism of action based on an oxygen-dependent entry into the bacterial cell and stasis of bacterial protein synthesis by binding to 30S ribosomal subunit [71]. These processes in turn lead to protein mistranslation and disintegration of the cytoplasmic membrane [72].

To assess the antibacterial potential of AgNPs and gentamicin loaded membranes, we performed a qrt-PCR, CFU assay, and agar diffusion tests. According to the review of Curtis et al., the gram-positive, facultative anaerobe, early colonizers *A. neaslundii* and *S. mutans* are the most prevalent bacteria within a healthy oral microbiota, thus, these strains were included in our investigation [60]. Furthermore, two anaerobe, gram-negative bacterial species were included: *F. nucleatum*, the second most prevalent intraoral microbe in health, and the periodontitis associated bacterial species *P. gingivalis* [73]. The utilization of artificial saliva provided optimal growth conditions for the bacteria with high similarity to natural clinical conditions of the oral cavity. The best antibacterial activity was observed for CM-Ag; consistently, the qrt-PCR results reflect the lowest bacterial DNA count for CM-Ag compared to all other material groups, indicating a reduced bacterial adhesion potential by 3log-steps compared to the control membranes (CM-C, CM-SSC, and NW-C). Similar results on sufficient antibacterial activity are reported by Dhas et al., showing Ag-loaded SF fibers with >90% inhibition against common skin infection associated with *P. aeruginosa* and *S. aureus* as well as ZOI results of >2 mm [74]. In another study, SS-based AgNP loaded films yielded ZOIs of >10 mm and markedly decreased colony

growth of *E. coli* and *S. aureus* compared to the non-functionalized controls [75]. Within the NWs group, the best antibacterial activity was shown in gentamicin-treated ones regarding viable and total bacterial count with a 2log-reduction in both categories (i.e., 99% reduction), and direct antibacterial activity with a ZOI of 7–8 mm. A possible explanation for the disparity between CM and NW findings lies within the manufacturing process of the SF and SS membranes. To functionalize CMs, aqueous AgNO3 or gentamicin were incorporated into the silk solution before the casting procedure. In contrast, for the modification of NWs, the active agents were incorporated into membranes after the electrospinning process. Another possible justification for the reduction in antibacterial activity can be the washing-out and/or interaction of silver ions (Ag ions) with components of the artificial saliva (e.g., BSA), culturing media (e.g., Hemin, Cysteine, Pepsin, etc.), or the PBS which used in the testing process. Ando et al. ascribed the compromise of the antibacterial activity of silver to components of the culturing media which contained fetal bovine serum (FBS) [76]. A main component of FBS is bovine serum albumin which was included in the artificial saliva of our tests (Section 2.4.1). On the other hand, gentamicin activity is shown to increase with the interaction of blood components (e.g., those included in CDC media), conforming with our results [76–78]. In many cases, the antibiotics entrapment can be affected by the internal conformation of polymer chains. In a study by Hassani Besheli et al. it was indicated that the loading of antibiotics can be enhanced by increasing the content of silk II (higher ß-sheet content) of matrices. Moreover, they proved that pH variations impact release kinetics of antibiotics from SF materials [79].

Some studies attribute an inherent bactericidal activity to the silk proteins fibroin and SS. For example, Bakhsheshi-Rad et al. found a ZOI of 3–3.5 mm for SS dressings on *E. coli* and *S. aureus* [80]. Other authors proved a positive correlation between colony growth inhibition and SS concentration [81]. SS mechanism of antibacterial action is supposed to be through membrane ballooning and bleb formation, which is a known mechanism for other antimicrobial peptides [82]. The inherent antibacterial property of SF is mainly reported as a result of its' barrier function as a wound dressing [83]. Additionally, SF has been associated with residual antimicrobial peptides (e.g., seroins) from the silk cocoons, which are natural protections of the silkworm against external pathogens [84]. Therefore, in this study, we assessed the possibility of an inherent antibacterial activity of the pristine silk proteins fibroin and sericin. Our results showed no antibacterial activity, neither with the SF and SS control membranes nor with the combined SF/SS membranes; however, they acted as a suitable mechanical barrier shown in the agar diffusion assay.

Our investigation has met different challenging points and limitations. In this study, we stored the samples in ethanol 70 v% solution and extracted them for an agar diffusion test. However, because of the antibacterial potency of the storage solution, we expected to have additional antibacterial effects and, subsequently, false-positive results. In order to eliminate errors associated with the storage conditions, we performed a simultaneous confirmatory test with a washing step in PBS before plating the samples onto the agar plate, which yielded similar results. Moreover, despite the oxygen dependent action of gentamicin, an anaerobic setting was necessary for proper bacterial colonization.

To sum up briefly, the investigated antibacterial silk protein-based membranes are promising substrates for wound healing applications in the field of oral and maxillofacial surgery. Future studies should be accomplished to further understand application specific material functionalization.

5. Conclusion

Silk proteins offer favorable characteristics that can be tailored to casted membranes or electro-spun nonwovens for the application as adherent/non-adherent wound dressings. The potential to alleviate infections can be realized through functionalization with antibacterial substances such as silver or gentamicin. The antibacterial activity of silver and silver loaded biomaterials has been described in literature thoroughly. In this study, we proved the antimicrobial effects of AgNPs and the aminoglycoside antibiotic gentamicin which was incorporated in silk protein membranes. Both functionalization methods proved containment of bacterial DNA count and colony growth of the common oral microbes *F. nucleatum*, *P. gingivalis*, *A. neaslundii*, and *S. mutans*. Prospective investigations should target on application specific material functionalization and understanding of in vivo effectivity in a suitable animal model.

Supplementary data to this article can be found online at https://doi.org/10.1016/j.bioadv.2022.212740.

CRediT authorship contribution statement

Schäfer S: bacterial analysis; design and planning of experiments; data collection; data analysis and interpretation of results; drafted the manuscript.

Smeets R: interpretation and critical revision; approval of the article.

Köpf M: idea and concept of the study; design and planning of experiments; interpretation of results; critical revision and approval of the article.

Drinic A: development of fabrication and functionalization methods for silk protein membranes as well as sample production; critical revision and approval of the article.

Kopp A: critical revision and approval of the article.

Kröger N: critical revision and approval of the article.

Hartjen P: cytocompatibility analysis; critical revision and approval of the article.

Assaf AT: interpretation; critical revision and approval of the article.

Aavani F: interpretation; critical revision and approval of the article.

Beikler T: critical revision and approval of the article.

Peters U: data collection, data analysis/interpretation.

Fiedler I: SEM analysis; data collection, critical revision and approval of the article.

Busse B: SEM analysis; data collection.

Stürmer EK: critical revision and approval of the article.

Vollkommer T: critical revision and approval of the article.

Gosau M: interpretation and critical revision; approval of the article.

Fuest S: interpretation; critical revision of the manuscript; approval of the article.

Declaration of competing interest

The authors declare that they have no conflict of interest to report.

Acknowledgements

The authors gratefully acknowledge Frank Fischer for his technical assistance culturing the bacterial strains, Thomas Derra for the graphical illustration of the antibacterial testing methods, and Eric Bibiza Freiwald for his assistance in the statistical data analysis.

References

[1] G. Broughton II, J.E. Janis, C.E. Attinger, The basic science of wound healing, Plast. Reconstr. Surg. 117 (7 Suppl) (2006) 12s–34s.
[2] G. Han, R. Ceilley, Chronic wound healing: a review of current management and treatments, Adv. Ther. 34 (3) (2017) 599–610.
[3] C. Politis, J. Schoenaers, R. Jacobs, J.O. Agbaje, Wound healing problems in the mouth, Front. Physiol. 7 (507) (2016).
[4] M. Waasdorp, B.P. Krom, F.J. Bikker, P.P. van Zuijlen, F.B. Niessen, S. Gibbs, The bigger picture: why oral mucosa heals better than skin, Biomolecules 11 (8) (2021) 1165.
[5] N. Funato, K. Moriyama, Y. Baba, T. Kuroda, Evidence for apoptosis induction in myofibroblasts during palatal mucoperiosteal repair, J. Dent. Res. 78 (9) (1999) 1511–1517.
[6] E.A. Yücel, O. Oral, V. Olgaç, C.K. Oral, Effects of fibrin glue on wound healing in oral cavity, J. Dent. 31 (8) (2003) 569–575.

[7] N.A.M. Barakat, M.A. Kanjwal, F.A. Sheikh, H.Y. Kim, Spider-net within the N6, PVA and PU electrospun nanofiber mats using salt addition: novel strategy in the electrospinning process, Polymer 50 (18) (2009) 4389–4396.

[8] R. Rauso, G.F. Nicoletti, E. Sesenna, C. Lo Faro, F. Chirico, R. Fragola, et al., Superficial temporal artery perforator flap: indications, surgical outcomes, and donor site morbidity, Dent. J. 8 (4) (2020) 117.

[9] F. Momen-Heravi, S.M. Peters, L. Garfinkle, P. Kang, Acellular dermal matrix as a barrier for guided bone regeneration of dehiscence defects around dental implants: a clinical and histological report, Implant. Dent. 27 (4) (2018) 521–524.

[10] K.C. Broussard, J.G. Powers, Wound dressings: selecting the most appropriate type, Am. J. Clin. Dermatol. 14 (6) (2013) 449–459.

[11] S. Alven, X. Nqoro, B.A. Aderibigbe, Polymer-based materials loaded with curcumin for wound healing applications, Polymers 12 (10) (2020) 2286.

[12] M. Rinastiti, Harijadi, A.L. Santoso, W. Sosroseno, Histological evaluation of rabbit gingival wound healing transplanted with human amniotic membrane, Int. J. Oral Maxillofac. Surg. 35 (3) (2006) 247–251.

[13] K. Ishikawa, Y. Ueyama, T. Mano, T. Koyama, K. Suzuki, T. Matsumura, Self-setting barrier membrane for guided tissue regeneration method: initial evaluation of alginate membrane made with sodium alginate and calcium chloride aqueous solutions, J. Biomed. Mater. Res. 47 (2) (1999) 111–115.

[14] Y. Ueyama, K. Ishikawa, T. Mano, T. Koyama, H. Nagatsuka, K. Suzuki, et al., Usefulness as guided bone regeneration membrane of the alginate membrane, Biomaterials 23 (9) (2002) 2027–2033.

[15] C. Xu, C. Lei, L. Meng, C. Wang, Y. Song, Chitosan as a barrier membrane material in periodontal tissue regeneration, J Biomed Mater Res B Appl Biomater 100 (5) (2012) 1435–1443.

[16] S. Zhang, Y. Huang, X. Yang, F. Mei, Q. Ma, G. Chen, et al., Gelatin nanofibrous membrane fabricated by electrospinning of aqueous gelatin solution for guided tissue regeneration, J. Biomed. Mater. Res. A 90 (3) (2009) 671–679.

[17] C. Holland, K. Numata, J. Rnjak-Kovacina, F.P. Seib, The biomedical use of silk: past, present, future, Adv. Healthc. Mater. 8 (1) (2019) 1800465.

[18] C. Sobajo, F. Behzad, X.F. Yuan, A. Bayat, Silk: a potential medium for tissue engineering, Eplasty 8 (2008), e47.

[19] P.P. Patil, M.R. Reagan, R.A. Bohara, Silk fibroin and silk-based biomaterial derivatives for ideal wound dressings, Int. J. Biol. Macromol. 164 (2020) 4613–4627.

[20] D. Chouhan, B.B. Mandal, Silk biomaterials in wound healing and skin regeneration therapeutics: from bench to bedside, Acta Biomater. 103 (2020) 24–51.

[21] M. Yonesi, M. Garcia-Nieto, G.V. Guinea, F. Panetsos, J. Pérez-Rigueiro, D. González-Nieto, Silk Fibroin: An Ancient Material for Repairing the Injured Nervous System, Pharmaceutics. 13 (3) (2021) 429, https://doi.org/10.3390/pharmaceutics13030429.

[22] M. Santin, A. Motta, G. Freddi, M. Cannas, In vitro evaluation of the inflammatory potential of the silk fibroin, J. Biomed. Mater. Res. 46 (3) (1999) 382–389.

[23] S. Napavichayanun, P. Aramwit, Effect of animal products and extracts on wound healing promotion in topical applications: a review, J. Biomater. Sci. Polym. Ed. 28 (8) (2017) 703–729.

[24] S.P. Miguel, D. Simões, A.F. Moreira, R.S. Sequeira, I.J. Correia, Production and characterization of electrospun silk fibroin based asymmetric membranes for wound dressing applications, Int. J. Biol. Macromol. 121 (2019) 524–535.

[25] M. Bienert, M. Hoss, M. Bartneck, S. Weinandy, M. Böbel, S. Jockenhövel, et al., Growth factor-functionalized silk membranes support wound healing in vitro, Biomed. Mater. 12 (4) (2017), 045023.

[26] Y. Zhang, L. Lu, Y. Chen, J. Wang, Y. Chen, C. Mao, et al., Polydopamine modification of silk fibroin membranes significantly promotes their wound healing effect, Biomaterials Science. 7 (12) (2019) 5232–5237.

[27] A. Oliveira, S. Simões, A. Ascenso, C.P. Reis, Therapeutic advances in wound healing, J. Dermatol. Treat. (2020) 1–21.

[28] L. Loomba, T. Scarabelli, Metallic nanoparticles and their medicinal potential. Part II: aluminosilicates, nanobiomagnets, quantum dots and cochleates, Ther. Deliv. 4 (9) (2013) 1179–1196.

[29] K.K. Wong, S.O. Cheung, L. Huang, J. Niu, C. Tao, C.M. Ho, et al., Further evidence of the anti-inflammatory effects of silver nanoparticles, ChemMedChem 4 (7) (2009) 1129–1135.

[30] Z.-m. Xiu, Q.-b. Zhang, H.L. Puppala, V.L. Colvin, P.J. Alvarez, Negligible particle-specific antibacterial activity of silver nanoparticles, Nano Lett. 12 (8) (2012) 4271–4275.

[31] E.M. Pritchard, T. Valentin, B. Panilaitis, F. Omenetto, D.L. Kaplan, Antibiotic-releasing silk biomaterials for infection prevention and treatment, Adv. Funct. Mater. 23 (7) (2013) 854–861.

[32] S.M. Dizaj, F. Lotfipour, M. Barzegar-Jalali, M.H. Zarrintan, K. Adibkia, Antimicrobial activity of the metals and metal oxide nanoparticles, Mater. Sci. Eng. C Mater. Biol. Appl. 44 (2014) 278–284.

[33] H.R. Rosen, A.P. Marczell, E. Czerwenka, M.O. Stierer, H. Spoula, H. Wasl, Local gentamicin application for perineal wound healing following abdominoperineal rectum excision, Am. J. Surg. 162 (5) (1991) 438–441.

[34] U. Gruessner, M. Clemens, P.V. Pahlplatz, P. Sperling, J. Witte, H.R. Rosen, et al., Improvement of perineal wound healing by local administration of gentamicin-impregnated collagen fleeces after abdominoperineal excision of rectal cancer, Am. J. Surg. 182 (5) (2001) 502–509.

[35] A. Kwong, J. Cogan, Y. Hou, R. Antaya, M. Hao, G. Kim, et al., Gentamicin induces laminin 332 and improves wound healing in junctional epidermolysis bullosa patients with nonsense mutations, Mol. Ther. 28 (5) (2020) 1327–1338.

[36] W. Zhou, Z. Jia, P. Xiong, J. Yan, Y. Li, M. Li, et al., Bioinspired and biomimetic AgNPs/gentamicin-embedded silk fibroin coatings for robust antibacterial and osteogenetic applications, ACS Appl. Mater. Interfaces 9 (31) (2017) 25830–25846.

[37] S. Schafer, H. Al-Qaddo, M. Gosau, R. Smeets, P. Hartjen, R.E. Friedrich, et al., Cytocompatibility of bone substitute materials and membranes, In Vivo 35 (4) (2021) 2035–2040.

[38] P. Gehrke, P. Hartjen, R. Smeets, M. Gosau, U. Peters, T. Beikler, et al., Marginal adaptation and microbial leakage at conometric prosthetic connections for implant-supported single crowns: an in vitro investigation, Int. J. Mol. Sci. 22 (2) (2021) 881.

[39] F. Carrouel, S. Viennot, J. Santamaria, P. Veber, D. Bourgeois, Quantitative molecular detection of 19 major pathogens in the interdental biofilm of periodontally healthy young adults, Front. Microbiol. 7 (2016) 840.

[40] T. Hoshino, M. Kawaguchi, N. Shimizu, N. Hoshino, T. Ooshima, T. Fujiwara, PCR detection and identification of oral streptococci in saliva samples using gtf genes, Diagn. Microbiol. Infect. Dis. 48 (3) (2004) 195–199.

[41] P.E. Kolenbrander, R.N. Andersen, D.S. Blehert, P.G. Egland, J.S. Foster, R. J. Palmer Jr., Communication among oral bacteria, Microbiol. Mol. Biol. Rev. 66 (3) (2002) 486–505, table of contents.

[42] B. Sampaio-Maia, I.M. Caldas, M.L. Pereira, D. Pérez-Mongiovi, R. Araujo, The oral microbiome in health and its implication in oral and systemic diseases, Adv. Appl. Microbiol. 97 (2016) 171–210.

[43] G.F. Rogers, A.A. Lim, J.B. Mulliken, B.L. Padwa, Effect of a syndromic diagnosis on mandibular size and sagittal position in Robin sequence, J. Oral Maxillofac. Surg. 67 (11) (2009) 2323–2331.

[44] S. Rastogi, M. Modi, B. Sathian, The efficacy of collagen membrane as a biodegradable wound dressing material for surgical defects of oral mucosa: a prospective study, J. Oral Maxillofac. Surg. 67 (8) (2009) 1600–1606.

[45] S. Omura, N. Mizuki, S. Horimoto, R. Kawabe, K. Fujita, A newly developed collagen/silicone bilayer membrane as a mucosal substitute: a preliminary report, Br. J. Oral Maxillofac. Surg. 35 (2) (1997) 85–91.

[46] D. Ryabova, N. Orlinskaya, S. Tsybusov, N. Homutinnikova, R. Lapshin, E. Durnovo, Application of polymer phospholipid matrix for closing open wounds on oral mucosa, СовреМенные технологии в Медицине 8 (1 (eng)) (2016).

[47] Ç. Kılıç, E.G.G. Peker, F. Acartürk, S.M.S. Kılıçaslan, Ş.Ç. Cevher, Investigation of the effects of local glutathione and chitosan administration on incisional oral mucosal wound healing in rabbits, Colloids Surf. B: Biointerfaces 112 (2013) 499–507.

[48] S.A. Ballestas, T.C. Turner, A. Kamalakar, Y.C. Stephenson, N.J. Willett, S. L. Goudy, et al., Improving hard palate wound healing using immune modulatory autotherapies, Acta Biomater. 91 (2019) 209–219.

[49] Y.S. Lim, S.K. Kwon, J.H. Park, C.G. Cho, S.W. Park, W.K. Kim, Enhanced mucosal healing with curcumin in animal oral ulcer model, Laryngoscope 126 (2) (2016) E68–E73.

[50] S. Yaprak Karavana, P. Güneri, G. Ertan, Benzydamine hydrochloride buccal bioadhesive gels designed for oral ulcers: preparation, rheological, textural, mucoadhesive and release properties, Pharm. Dev. Technol. 14 (6) (2009) 623–631.

[51] G. Lis, J. Zarzecka, J. Litwin, E. Jasek, T. Cichocki, J. Zapała, Effect of cultured autologous oral keratinocyte suspension in fibrin glue on oral wound healing in rabbits, Int. J. Oral Maxillofac. Surg. 41 (9) (2012) 1146–1152.

[52] M. Gholipourmalekabadi, S. Sapru, A. Samadikuchaksaraei, R.L. Reis, D.L. Kaplan, S.C. Kundu, Silk fibroin for skin injury repair: where do things stand? Adv. Drug Deliv. Rev. 153 (2020) 28–53.

[53] N. Kasoju, U. Bora, Silk fibroin in tissue engineering, Adv. Healthc. Mater. 1 (4) (2012) 393–412.

[54] J. Tang, Y. Han, F. Zhang, Z. Ge, X. Liu, Q. Lu, Buccal mucosa repair with electrospun silk fibroin matrix in a rat model, Int. J. Artif. Organs 38 (2) (2015) 105–112.

[55] Z. Ge, Q. Yang, X. Xiang, K.Z. Liu, Assessment of silk fibroin for the repair of buccal mucosa in a rat model, Int. J. Oral Maxillofac. Surg. 41 (5) (2012) 673–680.

[56] P. Kamalathevan, P.S. Ooi, Y.L. Loo, Silk-based biomaterials in cutaneous wound healing: a systematic review, Adv. Skin Wound Care 31 (12) (2018) 565–573.

[57] Q. Wang, S. Zhou, L. Wang, R. You, S. Yan, Q. Zhang, et al., Bioactive silk fibroin scaffold with nanoarchitecture for wound healing, Compos. Part B 224 (2021) 109165.

[58] M. Stevanović, M. Djošić, A. Janković, V. Kojić, M. Vukašinović-Sekulić, J. Stojanović, et al., Antibacterial graphene-based hydroxyapatite/chitosan coating with gentamicin for potential applications in bone tissue engineering, J. Biomed. Mater. Res. A 108 (11) (2020) 2175–2189.

[59] K.K. Panda, V.M.M. Achary, R. Krishnaveni, B.K. Padhi, S.N. Sarangi, S.N. Sahu, et al., In vitro biosynthesis and genotoxicity bioassay of silver nanoparticles using plants, Toxicol. in Vitro 25 (5) (2011) 1097–1105.

[60] M.J. Piao, K.A. Kang, I.K. Lee, H.S. Kim, S. Kim, J.Y. Choi, et al., Silver nanoparticles induce oxidative cell damage in human liver cells through inhibition of reduced glutathione and induction of mitochondria-involved apoptosis, Toxicol. Lett. 201 (1) (2011) 92–100.

[61] M. Składanowski, P. Golinska, K. Rudnicka, H. Dahm, M. Rai, Evaluation of cytotoxicity, immune compatibility and antibacterial activity of biogenic silver nanoparticles, Med. Microbiol. Immunol. 205 (6) (2016) 603–613.

[62] H. He, G. Tao, Y. Wang, R. Cai, P. Guo, L. Chen, et al., In situ green synthesis and characterization of sericin-silver nanoparticle composite with effective antibacterial activity and good biocompatibility, Mater. Sci. Eng. C Mater. Biol. Appl. 80 (2017) 509–516.

[63] X. Lv, H. Wang, A. Su, Y. Chu, A novel approach for sericin-conjugated silver nanoparticle synthesis and their potential as microbicide candidates, J. Microbiol. Biotechnol. 28 (8) (2018) 1367–1375.

[64] A. Gao, H. Chen, A. Hou, K. Xie, Efficient antimicrobial silk composites using synergistic effects of violacein and silver nanoparticles, Mater. Sci. Eng. C Mater. Biol. Appl. 103 (2019) 109821.
[65] M. Guzman, J. Dille, S. Godet, Synthesis and antibacterial activity of silver nanoparticles against gram-positive and gram-negative bacteria, Nanomedicine 8 (1) (2012) 37–45.
[66] L.D. Koh, J. Yeo, Y.Y. Lee, Q. Ong, M. Han, B.C. Tee, Advancing the frontiers of silk fibroin protein-based materials for futuristic electronics and clinical wound-healing (invited review), Mater. Sci. Eng. C Mater. Biol. Appl. 86 (2018) 151–172.
[67] M.D. Scherer, J.C.V. Sposito, W.F. Falco, A.B. Grisolia, L.H.C. Andrade, S.M. Lima, et al., Cytotoxic and genotoxic effects of silver nanoparticles on meristematic cells of Allium cepa roots: a close analysis of particle size dependence, Sci. Total Environ. 660 (2019) 459–467.
[68] H.J. Klasen, Historical review of the use of silver in the treatment of burns. I. Early uses, Burns 26 (2) (2000) 117–130.
[69] X. Lv, Z. Li, S. Chen, M. Xie, J. Huang, X. Peng, et al., Structural and functional evaluation of oxygenating keratin/silk fibroin scaffold and initial assessment of their potential for urethral tissue engineering, Biomaterials 84 (2016) 99–110.
[70] V. Gopinath, S. Priyadarshini, M. Loke, J. Arunkumar, E. Marsili, D. MubarakAli, et al., Biogenic synthesis, characterization of antibacterial silver nanoparticles and its cell cytotoxicity, Arab. J. Chem. 10 (2017) 1107–1117.
[71] X. Pan, S. Chen, D. Li, W. Rao, Y. Zheng, Z. Yang, et al., The synergistic antibacterial mechanism of gentamicin-loaded CaCO3 nanoparticles, Front. Chem. 5 (2018) 130.
[72] A.W. Serio, T. Keepers, L. Andrews, K.M. Krause, Aminoglycoside revival: review of a historically important class of antimicrobials undergoing rejuvenation, EcoSal Plus 8 (1) (2018).
[73] M.A. Curtis, P.I. Diaz, T.E. Van Dyke, The role of the microbiota in periodontal disease, Periodontol. 83 (1) (2020) 14–25.
[74] S.P. Dhas, S. Anbarasan, A. Mukherjee, N. Chandrasekaran, Biobased silver nanocolloid coating on silk fibers for prevention of post-surgical wound infections, Int. J. Nanomedicine 10 (Suppl. 1) (2015) 159–170.
[75] Y. Wang, R. Cai, G. Tao, P. Wang, H. Zuo, P. Zhao, et al., A novel AgNPs/sericin/agar film with enhanced mechanical property and antibacterial capability, Molecules 23 (7) (2018).
[76] Y. Ando, H. Miyamoto, I. Noda, F. Miyaji, T. Shimazaki, Y. Yonekura, et al., Effect of bacterial media on the evaluation of the antibacterial activity of a biomaterial containing inorganic antibacterial reagents or antibiotics, Biocontrol Sci. 15 (1) (2010) 15–19.
[77] A. Hostacká, Serum sensitivity and cell surface hydrophobicity of Klebsiella pneumoniae treated with gentamicin, tobramycin and amikacin, J. Basic Microbiol. 38 (5–6) (1998) 383–388.
[78] Y. Wang, J. Wang, S. Huang, C. Liu, Y. Fu, Evaluating the effect of aminoglycosides on the interaction between bovine serum albumins by atomic force microscopy, Int. J. Biol. Macromol. 134 (2019) 28–35.
[79] N. Hassani Besheli, F. Mottaghitalab, M. Eslami, M. Gholami, S.C. Kundu, D. L. Kaplan, et al., Sustainable release of vancomycin from silk fibroin nanoparticles for treating severe bone infection in rat tibia osteomyelitis model, ACS Appl. Mater. Interfaces 9 (6) (2017) 5128–5138.
[80] H.R. Bakhsheshi-Rad, A.F. Ismail, M. Aziz, M. Akbari, Z. Hadisi, M. Omidi, et al., Development of the PVA/CS nanofibers containing silk protein sericin as a wound dressing: in vitro and in vivo assessment, Int. J. Biol. Macromol. 149 (2020) 513–521.
[81] S. Gilotra, D. Chouhan, N. Bhardwaj, S.K. Nandi, B.B. Mandal, Potential of silk sericin based nanofibrous mats for wound dressing applications, Mater. Sci. Eng. C Mater. Biol. Appl. 90 (2018) 420–432.
[82] R. Xue, Y. Liu, Q. Zhang, C. Liang, H. Qin, P. Liu, et al., Shape changes and interaction mechanism of Escherichia coli cells treated with sericin and use of a sericin-based hydrogel for wound healing, Appl. Environ. Microbiol. 82 (15) (2016) 4663–4672.
[83] W. Zhang, L. Chen, J. Chen, L. Wang, X. Gui, J. Ran, et al., Silk fibroin biomaterial shows safe and effective wound healing in animal models and a randomized controlled clinical trial, Adv. Healthc. Mater. 6 (10) (2017).
[84] X. Guo, Z. Dong, Y. Zhang, Y. Li, H. Liu, Q. Xia, et al., Proteins in the cocoon of silkworm inhibit the growth of Beauveria bassiana, PLoS One 11 (3) (2016), e0151764.

2. Zusammenfassende Darstellung der Publikation

2.1 Einleitung

Die Wundheilung unterliegt einem komplexen molekularen Prozess, dessen grundlegende Schritte in allen Organsystemen des menschlichen Körpers konserviert sind. Dieser Prozess umfasst einen hochgradig orchestrierten Ablauf mit sich überschneidenden Phasen, die als Hämostase, Entzündung, Proliferation und Reparation bezeichnet werden (Broughton et al., 2006, Gurtner et al., 2008). Eine Vielzahl von Faktoren können diesen Prozess beeinflussen. Intrinsische Faktoren einschließlich der lokalen Bakterienflora, die Sauerstoff- und Gefäßversorgung des lokalen Gewebes sowie systemische Faktoren wie die psychische und physische Gesundheit des Patienten haben einen maßgeblichen Einfluss auf den Verlauf der Wundheilung (Politis et al., 2016). Vom Behandler beeinflussbar sind vor allem extrinsische Faktoren, die im Rahmen der Wundversorgung zu tragen kommen. Eine nicht ordnungsgemäße Versorgung der Wunde kann zu Schmerzen, Infektionen und unerwünschten Heilungserscheinungen wie eine Chronifizierung, Narbenbildung und Adhäsionen an das angrenzende Gewebe führen (Dunn et al., 2013, Guo und Dipietro, 2010). Insbesondere bei Wundheilungsstörungen im orofazialen Behandlungsbereich haben die Betroffenen einen hohen Leidensdruck und erfahren Einschränkungen der Lebensqualität. Chronische Wunden in diesem Bereich sind häufig auf eine pathologische Bakterienkolonisierung zurückzuführen, bei welchen Anaerobier einen erheblichen Anteil der mikrobiellen Population ausmachen (Bhattacharya et al., 2014). Durch ein Ungleichgewicht zwischen pathogenen und kommensalen Bakterien wird der Zustand der Homöostase in der Mundhöhle gestört und führt zur Schädigung von Weich- und Hartgewebe (Kolenbrander et al., 2002, Sampaio-Maia et al., 2016). Um eine solche Beeinträchtigungen zu vermeiden, müssen Biomaterialien für die Wundheilung eingesetzt werden, die das Wachstum pathogener Bakterien hemmen und gleichzeitig den Wundheilungsprozess fördern.

Je nach Ausmaß des Weichgewebsdefekts ist der Goldstandard in der Mund-, Kiefer- und Gesichtschirurgie die Verwendung autologer myokutaner Lappen oder allogener/xenogener Transplantate, z. B. azelluläre dermale Matrices (ADM). Autologe Lappenplastiken sind jedoch mit einer hohen Morbidität an der Entnahmestelle und unbefriedigenden kosmetischen Ergebnissen assoziiert, während ADMs nachweislich Entzündungsreaktionen und immunogene Reaktionen hervorrufen (Rauso et al., 2020, Momen-Heravi et al., 2018). Eines der bekanntesten Ansätze für die orale und faziale

Wundheilung ist die Anwendung von Membranen auf Polymerbasis. Hierbei erlangen neben den herkömmlichen Kollagenmaterialien, natürliche Biomaterialien auf Basis von Seidenproteinen große Aufmerksamkeit. Die aus Fibroin (70-80 %) und Sericin (20-30 %) bestehenden Makroproteine werden aus den Kokons der Seidenraupe *Bombyx mori* (*B. mori*) durch einen schonenden Löseprozess aus Salzen oder ionischen Detergentien in eine wässrige Lösung gebracht und können so als Ausgangsstoff für eine vielseitige Weiterverarbeitung (z. B. Fasern, Filme, Gele und dreidimensionale Gerüste) genutzt werden (Chouhan und Mandal, 2020). Diese gewannen aufgrund ihrer bemerkenswerten mechanischen Eigenschaften, ihrer überlegenen Biokompatibilität, ihrer Sauerstoff- und Wasserdampfdurchlässigkeit, ihrer kontrollierbaren proteolytischen Abbaubarkeit und ihrer minimalen Immunogenität zunehmend an Aufmerksamkeit in präklinischen und klinischen Studien (Holland et al., 2019, Zhang et al., 2017). Jüngste Studien zeigen, dass Fibroin und Sericin jede Phase des Wundheilungsprozesses ergänzen und daher in großem Umfang als Wundauflagen für die akute und chronische Wundheilung geeignet sind (Holland et al., 2019, Patil et al., 2020). Eine zusätzliche antibakterielle Aktivität, die auf die vorteilhaften Eigenschaften der Seidenproteine aufbaut, könnte die Anwendung dieser Biomaterialien in der Wundheilung maßgeblich erweitern. Trotz der experimentellen Bemühungen um die Entwicklung einer funktionalisierten Wundauflage, wurde die Anwendung von antibakteriell beladenen Seidenproteinmembranen für die orale und faziale Wundheilung bisher nicht untersucht. Daher haben wir in dieser In-vitro-Studie innovative antibakterielle Seidenproteinmembranen untersucht. Die Membranen (CM) und die Vliese (NW) wurden mit Silberionen/-nanopartikeln und Gentamicin funktionalisiert, wobei Gieß- und Elektrospinnverfahren zum Einsatz kamen. Ziel dieser Studie war die Evaluierung der antibakteriellen Eigenschaften der Membranen und Vliese für Wundheilungsanwendungen in der Mund-, Kiefer- und Gesichtschirurgie.

2.2 Material und Methoden

Für die Herstellung der Fibroin (SF) / Sericin (SS) -membranen und -vliese wurden *Bombyx mori* Seidenkokons zur Proteinextraktion der Firboin- und Sericinlösungen verwendet. Das Verfahren wurde nach der PureSilk®-Technologie der Firma Fibrothelium GmbH (Fibrothelium GmbH, Aachen, Deutschland) durchgeführt. Zwei Arten an Membranen wurden hergestellt: gegossene Membranen (CM) und

elektrogesponnene Vliese (NW). Zur Herstellung der gegossenen Membranen wurde zunächst die SF-Lösung mit der entsprechenden Funktionalisierungslösung (Gentamin oder Silbernitrat (AgNO3)) in eine PTFE-Form gegossen. Die Mischung aus AgNO3 und SF wurde zuvor eine Stunde lang UV-bestrahlt, um eine Silbernanopartikel (AgNP) Bildung zu induzieren. Nach 24-stündiger Trocknung bei 21 °C unter einer Abzugshaube hatten die fertigen CM eine Dicke von etwa 0,1 - 0,2 mm (Micromar 40 ER, Mahr GmbH, Deutschland). Zur Herstellung der Vliese wurde nach firmeninterner Technologie die SF-Lösung elektrogesponnen. In einem nächsten Schritt wurden die Vliese für etwa 60 Minuten in eine AgNO3-Lösung oder Gentamicinlösung getaucht. Die mit AgNO3 behandelten Vliese wurden ebenfalls UV-bestrahlt. Nach der Funktionalisierung standen fünf Variationen von gegossenen Membranen (Gentamicin, Silber, unbehandelte SF-Kontrollen, SF/SS Membranen und unbehandelte SS-Kontrollen) und drei Variationen von Vliesen (Gentamicin, Silber und unbehandelte SF-Kontrollen) zur weiteren Untersuchung zur Verfügung. Alle Proben wurden nach der Herstellung für eine Stunde im Ethanolbad (70 v%) nachbehandelt, um Hydrophobie zu erreichen. Abschließend wurden alle Materialien in Ethanol (70 v%) bei 4 °C gelagert. Die Oberflächenmorphologie der Proben wurde mit Hilfe des Rasterelektronenmikroskops (REM) (Crossbeam 340, Zeiss, Oberkochen, Deutschland) visualisiert. Vor der Aufnahme wurden die Proben sieben Tage lang unter einer Abzugshaube getrocknet. Mit einem Skalpell wurde anschließend im Bereich der Mittellinie jeder Proben ein Schnitt gesetzt, um Querschnittsabbildungen durchzuführen. Zur Gewährleistung der Elektronenstabilität wurden die Proben mit Gold besputtert (Sputter Coater S150B, Edwards, London, Vereinigtes Königreich). Die Bildgebung erfolgte im Sekundärelektronenmodus bei einer Beschleunigungsspannung von 5 kV, einem Arbeitsabstand von 5 mm und Vergrößerungen von 500 X bis 10.000 X. Die Untersuchung der Zytokompatibilität erfolgte in Anlehnung an unsere frühere Arbeit (37). Als toxisches Referenzmaterial für alle Tests dienten Polyurethanfolien mit 0,1 % Zinkdiethyldithiocarbamat (ZDEC) (Hatano Research Institute, Kanagawa, Japan). Für die indirekten Tests wurde das Zellkulturmedium als nicht toxische Kontrolle verwendet. Für den Live-Dead-Assay wurden Zellkulturdeckgläser (TCC) (Sarstedt, Nümbrecht, Deutschland, Kat. Nr. 83.1840.002) als nichttoxisches Kontrollmaterial verwendet. L929-Mausfibroblasten wurden von der European Collection of Cell Culture, ECACC (Salisbury, Vereinigtes Königreich) bezogen. Die Zellen wurden in MEM, das mit 10 % fötalem Rinderserum,

4 mM Glutamin und Penicillin/Streptomycin (jeweils 100 U/ml) (Life Technologies, Carlsbad, USA) ergänzt wurde bei 37 °C, 5 % CO2 und 95 % Luftfeuchtigkeit kultiviert. Die Zellen wurden bei 80 % Konfluenz passagiert. Für die Testung der Zellviabilität und Zytotoxität wurden das „Cell Proliferation Kit II“ (XTT) (Roche Diagnostics, Mannheim, Deutschland) und das „LDH-Cytotoxicity Assay Kit II" (BioVision, Milpitas, CA, USA) gemäß Herstelleranweisungen verwendet. Für den Live-Dead-Assay wurde zur Färbung der Membranproben 60 µl pro ml Medium Propidiumiodid (PI) -lösung (50 µg/ml in PBS) und 500 µl pro ml Medium Fluoresceindiacetat (FDA) -lösung (20 µg/ml in PBS aus 5 mg/ml FDA in Aceton-Stammlösung) in jedes Well einer 12-Well-Platte gegeben. Nach drei Minuten Inkubationszeit bei Raumtemperatur wurden die Proben mit PBS gespült und mittels Fluoreszenzmikroskop (Nikon ECLIPSE Ti-S/L100, Nikon GmbH, Düsseldorf, Deutschland) untersucht, welches mit einem Filter zur parallelen Detektion von roter und grüner Fluoreszenz ausgestattet war. Vor der antibakteriellen Testung wurden alle Proben in 70 v% Ethanol (EtOH) aufbewahrt, so dass sie als steril galten. Eine Stichprobengröße von N=10 pro Material (CM oder NW) und Funktionalisierung wurde für 24 h in künstlichen Speichel (a-Amylase 1 mg/ml, Mucin 0,85 mg/ml und bovines Serumalbumin (BSA) 0,4 mg/ml) inkubiert. Die Kultivierung der Bakterienstämme und die anschließende Behandlung der Proben erfolgte unter anaeroben Bedingungen bei 37 °C in einer Anaerobierbank (Whitley A35 Workstation Don Whitley Scientific, Bingley, Vereinigtes Königreich). Für eine flüssige Bakterienmischkultur wurden Ausstriche von frühkolonisierenden *Streptococcus mutans* (DSM 20523, DSMZ GmbH, Leibnitz, Deutschland), *Actinomyces naeslundii* (DSM 17233, DSMZ GmbH, Leibnitz, Deutschland), mittelkolonisierenden *Fusobacterium nucleatum* (DSM 15643, DSMZ GmbH, Leibnitz, Deutschland) und spätkolonisierenden *Porphyromonas gingivalis* (DSM 20709, DSMZ GmbH, Leibnitz, Deutschland) separat auf Blutagarplatten kultiviert und anschließend jeweils in ein flüssiges Nährmedium (CDC Anaerobe 5% Schafsblut) überführt. Nach ausreichender Inkubationszeit (2-5 Tagen) wurden 1 ml jedes Stammes in 20 ml CDC-Medium gemischt. Die optische Dichte (OD) der gemischten Bakterienkultur betrug 0,1. Die Testmembranen wurden in 24-Well-Platten mit je 1,5 ml Bakterienmischkultursuspension gelegt. Nach einer Inkubationszeit von 48 h wurden die Membranen separat in sterile 1,5 ml Eppendorfgefäße, welche mit PBS gefüllt waren, umgelagert, geschüttelt und aus jedem Eppendorfgefäß wurde 100 µl für die Bestimmung von Gesamt- und Lebendkeimzahl entnommen. Zur Bestimmung der

Gesamtkeimzahl wurden 50 µl der Probe mit einem DNA-Isolierungskit (innuPREP DNA Isolation Kit, Analytik Jena AG, Jena, Deutschland) aufgearbeitet und die DNA-Menge mittels quantitative Echtzeit-Polymerase-Kettenreaktion (qrt-PCR) (quantitative Real-Time-PCR, CFX96 Touch Real-Time PCR Detection System, Bio-Rad Laboratories, Berkeley, Kalifornien, USA) unter Verwendung eines universellen 16S-rRNA-Primers (HDA1GACTCCTACGGGAGGCAGCAGT,E1115RAGGGTTGCGCTCGTTGCGGG) und spezifischen Primern (s. Originalpublikation) bestimmt. Zur Bestimmung der Lebendkeimzahl wurde eine Colony Forming Unit (CFU) Analyse durchgeführt. Hierbei wurden 50 µl der Proben in einer Verdünnungsreihe (1:100, 1:1000, 1:10.000) auf Blutagarplatten ausgestrichen und die koloniebildenden Einheiten wurden gezählt. Des Weiteren wurde ein Hemmhoftest/Agar-Diffusionstest durchgeführt. Hierbei wurden für jedes Material fünf Blutagarplatten mit der Mischkultur oder eines der Bakterienkulturen beimpft und zwei Proben je Material auf eine Platte gelegt. Nach einer Bebrütungszeit von 24 h wurden die jeweiligen Hemmhöfe mit einem Millimetermaß gemessen. Für die statistische Datenauswertung der Zytokompatibilitätstests wurde die mittlere Extinktion der Blindkontrollen ohne Zellen von den mittleren Extinktionen der Proben subtrahiert und die Daten als Prozentwert der Negativkontrolle angegeben. Die statistische Auswertung der antibakteriellen Tests wurde mit SAS 7.4 (SAS Institute Inc., Cary, North Carolina, USA) durchgeführt. Die mittleren bakteriellen DNA-Mengen aus der qrt-PCR-Messung und die CFU-Analysewerte wurden ausgewertet. Für die qrt-PCR- und CFU-Analyseergebnisse wurde ein exponentiell-lineares Modell gewählt. P-Werte < 0,05 wurden als statistisch signifikant angesehen.

2.3 Ergebnisse

Die rasterelektronenmikroskopischen Aufnahmen stellen die hochporöse Struktur der verwobenen Vliese im Vergleich zu der glatten Oberfläche der Gussmembranen dar. In Querschnittsaufnahmen konnte die aufrechterhaltene Kontinuität der Faserverbindungen über die gesamte Dicke der Vliese visualisiert werden (s. Abb. 2, Originalpublikation).

Alle Proben wiesen eine anwendungsgerechte Biokompatibilität auf. Mit Ausnahme der silberbeladenen Materialien (CM-Ag, NW-Ag) erzielten alle Membranen Viabilitätswerte > 70% der Negativkontrolle im indirekten Assay, welche gemäß DIN

EN ISO 10993-5:2009 (Deutsches Institut für Normung, Berlin, Deutschland) nicht-toxisch ist. Die Viabilität war bei allen Materialien ähnlich (91% - 108% der Negativkontrolle) mit Ausnahme der silberbeladenen Proben (4% der Negativkontrolle) ($p < 0,001$) (s. Abb. 3, Originalpublikation). Die Zytotoxizitätswerte waren für alle Proben außer für silberbeladene Proben konstant im Bereich der Negativkontrolle (Zellen, die mit Zellkulturmedium inkubiert wurden) (s. Abb. 4, Originalpublikation). Auffällig war, dass die silberbeladenen Proben negative Werte im LDH-Assay anzeigten, sodass der Verdacht bestand, Silbernanopartikel/-ionen könnten den Assay stören. Daher wurde ein Test auf Assay-Interferenz durchgeführt, welcher eine Teststörung durch die Silberionen und somit falsch negative Zytotoxizitätswerte für die silberbeladenen Materialien ergab. Im Live-Dead-Assay wurde für alle Proben eine Vielzahl grüner, FDA-positiver, vitaler Zellen nachgewiesen (s. Abb. 5, Originalpublikation). Nur vereinzelten konnten rote, PI-positive, tote Zellen mit Ausnahme der silberbeladenen Proben nachgewiesen werden. Insgesamt fielen die Biokompatibilitätstests positiv für alle Materialien aus mit Ausnahme der silberhaltigen Proben, welche weniger positive Ergebnisse erzielten. Die Lebendkeimzahl bestimmt durch die CFU-Analyse ergab ein signifikant niedriges Koloniewachstum für CM-Ag ($p < 0,0001$) im Vergleich zu allen anderen Gruppen, gefolgt von CM-G und NW-G ($p < 0,02$) (s. Abb. 6, Originalpublikation). CM-Ag verringerte die bakterielle DNA-Menge um 3 log Stufen im Vergleich zu der Positivkontrolle (bakterielle Mischkulturlösung), welches mit einer Reduktion von 99,9 % gleichzusetzen ist. Zwischen CM-G und NW-G konnte kein signifikanter Unterschied festgestellt werden. NW-Ag zeigte ähnliche CFU-Werte wie die Kontrolle NW-C ($p = 0,7$). CM-SF/SS und die Kontrollen CM-SSC und CM-C wiesen mit $p = 0,9$ und $p = 0,6$ CFU-Werte in einem ähnlichen Bereich auf. Alle getesteten Materialien wiesen im Vergleich zur Positivkontrolle (bakterielle Mischkulturlösung) signifikant niedrigere CFU-Werte auf ($p < 0,0001$). Insgesamt wurde die bakterielle Viabilität in folgender Reihenfolge am effektivsten eingedämmt: CM-Ag, NW-G, CM-G, NW-Ag, NW-C, CM-C, CM-SSC, und CM-SF/SS. Die Gesamtkeimzahl wurde anhand der Menge der Bakterien-DNA im qrt-PCR erfasst (s. Abb. 7, Originalpublikation). Dabei wiesen alle getesteten Membranen im Vergleich zur Positivkontrolle signifikant niedrigere DNA-Mengen auf ($p < 0,0001$). Die niedrigste DNA-Menge war für CM-Ag unter allen Vergleichsgruppen zu verzeichnen ($p < 0,0001$). CM-Ag verringerte die bakterielle DNA-Menge um 3 log Stufen oder um 99,9 % im Vergleich zur Positivkontrolle. In Übereinstimmung mit den CFU-Ergebnissen

wurde kein statistischer Unterschied zwischen CM-G und NW-G festgestellt ($p = 0,1$). Im Gegensatz zu den CFU-Ergebnissen wies NW-Ag im Vergleich zur Kontrolle NW-C deutlich weniger bakterielle DNA auf ($p < 0,005$), welches auf eine Eindämmung der Gesamtkeimzahl hinweist. Insgesamt wurde die Gesamtkeimzahl in folgender Reihenfolge am effektivsten verringert: CM-Ag, NW-G, CM-G, NW-Ag, NW-C, CM-C, CM-SSC, und CM-SF/SS. Im Hemmhoftest wurde für beide Materialtypen, gegossene Membranen und Vliese, der größte Hemmhofdurchmesser von 7-8 mm für Gentamicinproben (CM-G, NW-G) und der zweitgrößte Hemmhofdurchmesser von 2-3 mm für silberbeladene Proben (CM-Ag, NW-Ag) festgestellt (s. Abb. 8, Originalpublikation). Bei den unbehandelten Kontrollen (CM-C, CM-SSC, NW-C) wurde kein Hemmhof festgestellt. Entsprechend ergaben auch die kombinierten SF/SS-Membranen keinen Hemmhof. Insgesamt konnte bei gentamicinbeladenen Membranen gefolgt von silberbeladenen Membranen die ausgeprägteste direkte antibakterielle Aktivität gefunden werden.

2.4 Diskussion

Die Auswahl eines vielseitigen biokompatiblen Materials ist eines der größten Herausforderungen auf dem Gebiet der orofazialen Wundheilung, da das Zielgewebe sensibel und aufgrund der Nähe zur bakteriendichten Mundflora anfällig für postoperative Infektionen ist. Bislang galten Biomaterialien auf Basis von Kollagen als vielversprechende Biopolymere zur Herstellung resorbierbarer Wundauflagen. In einer klinischen Studie von Rastogi et al. wurden bei 60 Patienten nach Exzision prämaligner Läsionen an der Mundschleimhaut und nach Inzisionsbiopsiewunden im orofazialen Bereich bovine dezellularisierte Kollagenmembranen erfolgreich verwendet (Rastogi et al., 2009). In einer ähnlichen klinischen Studie setzten Omura et al. Kollagenmembranen bei fünf Patienten nach operativen Tumorexzision ein und beobachten eine Regeneration des nativen Bindegewebes nach 4-5 Wochen (Omura et al., 1997). Nichtsdestotrotz zeigen andere Studien, dass Materialien xenogenen Ursprungs wie das Kollagen immunogene Reaktionen auslösen und durch Kollagenolyse eine Entzündung mit Zerstörung des umliegenden Gewebes begünstigen (Badylak and Gilbert, 2008, Cheng et al., 2014). Dies hat nicht nur sozioökonomische Risiken wie eine verlängerte Krankheitsdauer und die Notwendigkeit einer Zweitoperation zur Folge, sondern ist auch mit einer erhöhten Mortalität assoziiert. Daher bedarf es, den Fokus auf alternative natürliche

Biomaterialien in der Wundheilung zu lenken. Aufgrund der einzigartigen Eigenschaften der Seidenproteine Fibroin und Sericin untersuchten wir in dieser Studie innovative antibakterielle Membranen und Vliese aus Fibroin- und Sericinextrakten, funktionalisiert mit Silberionen oder Gentamicin, auf Anwendbarkeit für die antibakterielle Wundheilung in der Mund-, Kiefer- und Gesichtschirurgie. Zunächst ist es für eine Wundauflage notwendig, im lokalen Gewebe die Reparation und Regeneration nativer Zellen zu unterstützen und zu fördern. Es ist erwiesen, dass Nanofaserstrukturen aus Seide eine bessere Anheftung und Proliferation von Fibroblasten und Keratinozyten ermöglichen als andere kommerzielle Wundauflagen und somit den Heilungsprozess von Wunden in Haut und Schleimhaut verbessern (Gholipourmalekabadi et al., 2020, Kasoju and Bora, 2012). Tang et al. testeten die Wundheilungsfähigkeit von elektrogesponnenen SF-Vliesen auf der Wangenschleimhaut von Ratten und zeigten, dass SF-Vliese den Heilungsprozess fördern und eine entzündungshemmende Wirtsreaktionen induzieren (Tang et al., 2015). Zudem konnten Biomaterialien auf Seidenbasis eine ausgezeichnete Biokompatibilität zeigen, da sie die Viabilität und Proliferation von humanen MC3T3-Osteoblasten fördern (Kamalathevan et al., 2018, Wang et al., 2021). In dieser Studie wurde die Biokompatibilität der SF und SS Membranen mittels XTT-, LDH- und Live-Dead-Assay an L929-Mausfibroblasten untersucht. Die Ergebnisse des XTT- und LDH-Tests zeigen eine gute Zytokompatibilität für alle nicht funktionalisierten Membranen und mit Gentamicin modifizierten Membranen. Diese Ergebnisse veranschaulichen eine sichere, tolerierbare Anwendungsdosis von 10 mg/ml Gentamicin für L929-Mausfibroblasten. Ähnliche Ergebnisse erzielten Stevanovic et al. die für L929-Zellen gut verträgliche Gentamicinkonzentrationen von weniger als 50 mg/ml nachweisen konnten (Stevanović et al., 2020). Im Gegensatz dazu verringerten Gussmembranen und Vliese funktionalisiert mit AgNO3 die Proliferation von L929-Zelllinie im XTT-Assay und zeigten Zytotoxizität im LDH-Assay sowie im Live-Dead-Assay. Die meisten Studien berichten über eine sichere, nicht zytotoxische Anwendung von AgNPs bei Konzentrationen von ≤ 25 mg/L (He et al., 2017, Lv et al., 2018). In unserer Studie betrug die Konzentration der AgNO3 Fuktionalisierungslösung 100 mg/L, welche eine Erklärung für die erhöhte Zytotoxizität geben kann. Zudem korreliert die Zytotoxizität von Silbernanopartikeln (AgNP), die nach UV-Bestrahlung entstanden sind, auch umgekehrt proportional mit der Größe der Nanopartikel, sodass die Zytotoxizität mit zunehmender Partikelgröße aufgrund des

geringeren Verhältnisses von Oberfläche zu Volumen abnimmt (Gao et al., 2019, Guzman et al., 2012, Koh et al., 2018, Scherer et al., 2019). Die Verwendung von Silber als antibakterielle Substanz in der regenerativen Medizin wird schon seit Jahrzehnten untersucht (Klasen, 2000, Lv et al., 2016). Es wurde festgestellt, dass die antibakterielle Wirkung von Silber auf eine Störung der Membranpermeabilität beruht, die zum Verlust von intrazellulären K+-Ionen, ATP und Phospholipiden führt. Darüber hinaus verursachen Silbernanopartikel oxidative Schäden, indem reaktive Sauerstoffspezies (ROS) produziert werden und dadurch intrazelluläre Metabolite durch die permeabilisierte Membran austreten können (Gopinath et al., 2017). Der Wirkmechanismus des Aminoglykosid-Antibiotikums Gentamicin hingegen beruht auf ein sauerstoffabhängiges Eindringen in die Bakterienzelle und einer Blockierung der 30S ribosomalen Untereinheit der bakteriellen Proteinbiosynthese (Pan et al., 2017). Dieser Prozess führt zu einer Fehltranslation von Proteinen und zum Zerfall der Zytoplasmamembran (Serio et al., 2018).

Das Hauptziel dieser Studie war, eine antibakterielle Aktivität bei den mit AgNP und gentamicinfunktionalisierten Membranen zu induzieren. Um das antibakterielle Potenzial von AgNPs und mit gentamicinbeladenen Membranen zu bewerten, führten wir eine qrt-PCR Untersuchung, CFU-Assays und Agar-Diffusionstests durch mit einer Auswahl an typischen Repräsentanten der oralen Mikrobiota.

Dem systematischen Review von Curtis et al. nach sind die grampositiven, fakultativ anaeroben, frühkolonisierenden *A. neaslundii* und *S. mutans* die am weitesten verbreiteten Bakterien in einer gesunden oralen Mikrobiota, weshalb diese Stämme in unsere Untersuchung einbezogen wurden (Piao et al., 2011). Außerdem wurden zwei anaerobe, gramnegative Bakterienarten einbezogen: *F. nucleatum*, der zweithäufigste intraorale Bakterienstamm bei Gesunden, und die mit Parodontitis assoziierte Bakterienart *P. gingivalis* (Curtis et al., 2020). Die Verwendung von künstlichem Speichel bot optimale Wachstumsbedingungen für die Bakterien, die den klinischen Bedingungen in der Mundhöhle sehr ähnlich sind. Die beste antibakterielle Aktivität wurde für silberbeladene Gussmembranen (CM-Ag) sowohl in Bezug auf die Verringerung der Viabilität als auch auf die Bakterien-DNA-Menge beobachtet. Die qrt-PCR-Ergebnisse spiegelten für CM-Ag im Vergleich zu den Kontrollmembranen (CM-C, CM-SSC und NW-C) eine um 3 log Stufen reduzierte bakterielle DNA-Menge wider, die als Verringerung des Adhäsionspotenzials der Bakterien interpretiert werden kann. Ähnliche Ergebnisse zu Ag-beladenen SF-Fasern werden von Dhas et al. berichtet,

die eine Hemmung von > 90 % gegen häufige Hautinfektionen im Zusammenhang mit *P. aeruginosa* und *S. aureus* sowie ZOI-Ergebnisse von > 2 mm zeigen (Dhas et al., 2015). Auch in unserer Studie erreichten mit Silber funktionalisierte Membranen einen Hemmhof von 2-3 mm. Innerhalb der Vlies-Gruppe zeigten die mit funktionalisierten Membranen die beste antibakterielle Aktivität sowohl bei der Verringerung der DNA-Menge als auch in der CFU-Analyse mit einer 2 log Stufen Reduktion in beiden Kategorien (d. h. 99 % Reduktion). Im Hemmhoftest konnten die mit gentamicinfunktionalisierten Materialien (CM-G und NW-G) die beste antibakterielle Aktivität mit einem ZOI von 7 - 8 mm im Vergleich zu allen anderen Kontrollmembranen zeigen. Eine mögliche Erklärung für die Diskrepanz zwischen der antibakteriellen Aktivität von Silber und Gentamicin innerhalb der unterschiedlichen Materialtypen liegt im Herstellungsprozess der Membranen. Für die Funktionalisierung der CMs wurden der Seidenlösung vor dem Gießvorgang flüssiges AgNO3 oder Gentamicin zugesetzt. Im Gegensatz dazu wurden die Vliese nach dem Elektrospinnverfahren in die Funktionalisierungslösung eingetaucht. So kann ein möglicher Grund für die Verringerung der antibakteriellen Aktivität das Auswaschen und/oder die Wechselwirkung von Silberionen (Ag-Ionen) in den Vliesen mit Bestandteilen des künstlichen Speichels (z. B. BSA), der Kulturmedien (z. B. Hemin, Cystein, Pepsin usw.) oder des PBS sein. Beispielsweise führten Ando et al. (2010) die Beeinträchtigung der antibakteriellen Aktivität von silberbeladenen SF-Vliesen auf Bestandteile der Kulturmedien zurück, die fötales Kälberserum (FKS) enthielten. Ein Hauptbestandteil von FKS ist bovines Serumalbumin, das in dem von uns verwendeten künstlichen Speichel enthalten war. Andererseits ist in der Literatur beschrieben, dass die Aktivität von Gentamicin durch Wechselwirkung mit Blutkomponenten (z. B. in CDC-Medien) zunimmt, welche mit unseren Ergebnissen für die NW-Gs übereinstimmt (Ando et al., 2010, Hostacká, 1998, Wang et al., 2019). Zudem kann in vielen Fällen der Einschluss von Antibiotika durch die interne Konformation der SF-Polymerketten beeinflusst werden. In einer Studie von Hassani Besheli et al. wurde gezeigt, dass eine Beladung von elektrogesponnen Vliesen mit Antibiotika durch eine Erhöhung des Gehalts an Seide II (höherer ß-Faltblatt-Gehalt) verbessert werden kann. Außerdem wiesen sie nach, dass pH-Variationen die Freisetzungskinetik von Antibiotika aus SF-Materialien beeinflussen (Hassani Besheli et al., 2017).

.

2.5 Schlussfolgerung

Die ideale Wundauflage ist hydrophil, sauerstoffdurchlässig, saugfähig, biokompatibel, biologisch abbaubar und zu guter Letzt: sie schützt die Wunde vor Infektionen und Mikroorganismen. Biomaterialien auf Seidenproteinbasis bieten natürlicherweise all jene Struktur- und Funktionseigenschaften, die eine ideale Wundauflage benötigt. Mit der Ausnahmeder einer inhärenten antibakteriellen Wirksamkeit. In dieser Studie nutzten wir die vorteilhaften mechanischen Eigenschaften der Seidenproteine und evaluierten neuartige antibakteriell funktionalisierte Seidenmembranen und -vliese. Die auf die typischen oralen Bakterien getesteten Silber- und Gentamicinmembranen/ -vliese zeigten eine vielversprechende antibakterielle Wirksamkeit. Sodass entsprechend der Ergebnisse dieser Studie davon ausgegangen werden kann, dass der Einsatz der getesteten Membranen und Vliese als Wundheilungsmaterial im Bereich der Mund-, Kiefer- und Gesichtschirurgie geeignet ist. Zukünftig sollten Studien zur Optimierung der Materialbeladung sowie Studien mit in vivo Wundmodellen die aktuellen Ergebnisse ergänzen.

2.6 Literaturverzeichnis

ANDO, Y., MIYAMOTO, H., NODA, I., MIYAJI, F., SHIMAZAKI, T., YONEKURA, Y., MIYAZAKI, M., MAWATARI, M. & HOTOKEBUCHI, T. 2010. Effect of bacterial media on the evaluation of the antibacterial activity of a biomaterial containing inorganic antibacterial reagents or antibiotics. *Biocontrol Sci,* 15**,** 15-9.

BADYLAK, S. F. & GILBERT, T. W. 2008. Immune response to biologic scaffold materials. *Semin Immunol,* 20**,** 109-16.

BHATTACHARYA, R., XU, F., DONG, G., LI, S., TIAN, C., PONUGOTI, B. & GRAVES, D. T. 2014. Effect of bacteria on the wound healing behavior of oral epithelial cells. *PLoS One,* 9**,** e89475.

BROUGHTON, G., 2ND, JANIS, J. E. & ATTINGER, C. E. 2006. The basic science of wound healing. *Plast Reconstr Surg,* 117**,** 12s-34s.

CHENG, C. W., SOLORIO, L. D. & ALSBERG, E. 2014. Decellularized tissue and cell-derived extracellular matrices as scaffolds for orthopaedic tissue engineering. *Biotechnol Adv,* 32**,** 462-84.

CHOUHAN, D. & MANDAL, B. B. 2020. Silk biomaterials in wound healing and skin regeneration therapeutics: From bench to bedside. *Acta Biomater,* 103**,** 24-51.

CURTIS, M. A., DIAZ, P. I. & VAN DYKE, T. E. 2020. The role of the microbiota in periodontal disease. *Periodontol 2000,* 83**,** 14-25.

DHAS, S. P., ANBARASAN, S., MUKHERJEE, A. & CHANDRASEKARAN, N. 2015. Biobased silver nanocolloid coating on silk fibers for prevention of post-surgical wound infections. *Int J Nanomedicine,* 10 Suppl 1**,** 159-70.

DUNN, L., PROSSER, H. C., TAN, J. T., VANAGS, L. Z., NG, M. K. & BURSILL, C. A. 2013. Murine model of wound healing. *J Vis Exp***,** e50265.

GAO, A., CHEN, H., HOU, A. & XIE, K. 2019. Efficient antimicrobial silk composites using synergistic effects of violacein and silver nanoparticles. *Mater Sci Eng C Mater Biol Appl,* 103**,** 109821.
GHOLIPOURMALEKABADI, M., SAPRU, S., SAMADIKUCHAKSARAEI, A., REIS, R. L., KAPLAN, D. L. & KUNDU, S. C. 2020. Silk fibroin for skin injury repair: Where do things stand? *Adv Drug Deliv Rev,* 153**,** 28-53.
GOPINATH, V., PRIYADARSHINI, S., LOKE, M. F., ARUNKUMAR, J., MARSILI, E., MUBARAKALI, D., VELUSAMY, P. & VADIVELU, J. 2017. Biogenic synthesis, characterization of antibacterial silver nanoparticles and its cell cytotoxicity. *Arabian Journal of Chemistry,* 10**,** 1107-1117.
GUO, S. & DIPIETRO, L. A. 2010. Factors affecting wound healing. *J Dent Res,* 89**,** 219-29.
GURTNER, G. C., WERNER, S., BARRANDON, Y. & LONGAKER, M. T. 2008. Wound repair and regeneration. *Nature,* 453**,** 314-21.
GUZMAN, M., DILLE, J. & GODET, S. 2012. Synthesis and antibacterial activity of silver nanoparticles against gram-positive and gram-negative bacteria. *Nanomedicine,* 8**,** 37-45.
HASSANI BESHELI, N., MOTTAGHITALAB, F., ESLAMI, M., GHOLAMI, M., KUNDU, S. C., KAPLAN, D. L. & FAROKHI, M. 2017. Sustainable Release of Vancomycin from Silk Fibroin Nanoparticles for Treating Severe Bone Infection in Rat Tibia Osteomyelitis Model. *ACS Appl Mater Interfaces,* 9**,** 5128-5138.
HE, H., TAO, G., WANG, Y., CAI, R., GUO, P., CHEN, L., ZUO, H., ZHAO, P. & XIA, Q. 2017. In situ green synthesis and characterization of sericin-silver nanoparticle composite with effective antibacterial activity and good biocompatibility. *Mater Sci Eng C Mater Biol Appl,* 80**,** 509-516.
HOLLAND, C., NUMATA, K., RNJAK-KOVACINA, J. & SEIB, F. P. 2019. The Biomedical Use of Silk: Past, Present, Future. *Adv Healthc Mater,* 8**,** e1800465.
HOSTACKÁ, A. 1998. Serum sensitivity and cell surface hydrophobicity of Klebsiella pneumoniae treated with gentamicin, tobramycin and amikacin. *J Basic Microbiol,* 38**,** 383-8.
KAMALATHEVAN, P., OOI, P. S. & LOO, Y. L. 2018. Silk-Based Biomaterials in Cutaneous Wound Healing: A Systematic Review. *Adv Skin Wound Care,* 31**,** 565-573.
KASOJU, N. & BORA, U. 2012. Silk fibroin in tissue engineering. *Adv Healthc Mater,* 1**,** 393-412.
KLASEN, H. J. 2000. Historical review of the use of silver in the treatment of burns. I. Early uses. *Burns,* 26**,** 117-30.
KOH, L. D., YEO, J., LEE, Y. Y., ONG, Q., HAN, M. & TEE, B. C. 2018. Advancing the frontiers of silk fibroin protein-based materials for futuristic electronics and clinical wound-healing (Invited review). *Mater Sci Eng C Mater Biol Appl,* 86**,** 151-172.
KOLENBRANDER, P. E., ANDERSEN, R. N., BLEHERT, D. S., EGLAND, P. G., FOSTER, J. S. & PALMER, R. J., JR. 2002. Communication among oral bacteria. *Microbiol Mol Biol Rev,* 66**,** 486-505, table of contents.
LV, X., LI, Z., CHEN, S., XIE, M., HUANG, J., PENG, X., YANG, R., WANG, H., XU, Y. & FENG, C. 2016. Structural and functional evaluation of oxygenating keratin/silk fibroin scaffold and initial assessment of their potential for urethral tissue engineering. *Biomaterials,* 84**,** 99-110.

LV, X., WANG, H., SU, A. & CHU, Y. 2018. A Novel Approach for Sericin-Conjugated Silver Nanoparticle Synthesis and Their Potential as Microbicide Candidates. *J Microbiol Biotechnol,* 28**,** 1367-1375.

MOMEN-HERAVI, F., PETERS, S. M., GARFINKLE, L. & KANG, P. 2018. Acellular Dermal Matrix as a Barrier for Guided Bone Regeneration of Dehiscence Defects Around Dental Implants: A Clinical and Histological Report. *Implant Dent,* 27**,** 521-524.

OMURA, S., MIZUKI, N., HORIMOTO, S., KAWABE, R. & FUJITA, K. 1997. A newly developed collagen/silicone bilayer membrane as a mucosal substitute: a preliminary report. *British Journal of Oral and Maxillofacial Surgery,* 35**,** 85-91.

PAN, X., CHEN, S., LI, D., RAO, W., ZHENG, Y., YANG, Z., LI, L., GUAN, X. & CHEN, Z. 2017. The Synergistic Antibacterial Mechanism of Gentamicin-Loaded CaCO (3) Nanoparticles. *Front Chem,* 5**,** 130.

PATIL, P. P., REAGAN, M. R. & BOHARA, R. A. 2020. Silk fibroin and silk-based biomaterial derivatives for ideal wound dressings. *Int J Biol Macromol,* 164**,** 4613-4627.

PIAO, M. J., KANG, K. A., LEE, I. K., KIM, H. S., KIM, S., CHOI, J. Y., CHOI, J. & HYUN, J. W. 2011. Silver nanoparticles induce oxidative cell damage in human liver cells through inhibition of reduced glutathione and induction of mitochondria-involved apoptosis. *Toxicol Lett,* 201**,** 92-100.

POLITIS, C., SCHOENAERS, J., JACOBS, R. & AGBAJE, J. O. 2016. Wound Healing Problems in the Mouth. *Front Physiol,* 7**,** 507.

RASTOGI, S., MODI, M. & SATHIAN, B. 2009. The efficacy of collagen membrane as a biodegradable wound dressing material for surgical defects of oral mucosa: a prospective study. *J Oral Maxillofac Surg,* 67**,** 1600-6.

RAUSO, R., NICOLETTI, G. F., SESENNA, E., LO FARO, C., CHIRICO, F., FRAGOLA, R., LO GIUDICE, G. & TARTARO, G. 2020. Superficial Temporal Artery Perforator Flap: Indications, Surgical Outcomes, and Donor Site Morbidity. *Dent J (Basel),* 8.

SAMPAIO-MAIA, B., CALDAS, I. M., PEREIRA, M. L., PÉREZ-MONGIOVI, D. & ARAUJO, R. 2016. The Oral Microbiome in Health and Its Implication in Oral and Systemic Diseases. *Adv Appl Microbiol,* 97**,** 171-210.

SCHERER, M. D., SPOSITO, J. C. V., FALCO, W. F., GRISOLIA, A. B., ANDRADE, L. H. C., LIMA, S. M., MACHADO, G., NASCIMENTO, V. A., GONÇALVES, D. A., WENDER, H., OLIVEIRA, S. L. & CAIRES, A. R. L. 2019. Cytotoxic and genotoxic effects of silver nanoparticles on meristematic cells of Allium cepa roots: A close analysis of particle size dependence. *Sci Total Environ,* 660**,** 459-467.

SERIO, A. W., KEEPERS, T., ANDREWS, L. & KRAUSE, K. M. 2018. Aminoglycoside Revival: Review of a Historically Important Class of Antimicrobials Undergoing Rejuvenation. *EcoSal Plus,* 8.

STEVANOVIĆ, M., DJOŠIĆ, M., JANKOVIĆ, A., KOJIĆ, V., VUKAŠINOVIĆ-SEKULIĆ, M., STOJANOVIĆ, J., ODOVIĆ, J., CREVAR SAKAČ, M., KYONG YOP, R. & MIŠKOVIĆ-STANKOVIĆ, V. 2020. Antibacterial graphene-based hydroxyapatite/chitosan coating with gentamicin for potential applications in bone tissue engineering. *J Biomed Mater Res A,* 108**,** 2175-2189.

TANG, J., HAN, Y., ZHANG, F., GE, Z., LIU, X. & LU, Q. 2015. Buccal mucosa repair with electrospun silk fibroin matrix in a rat model. *Int J Artif Organs,* 38**,** 105-12.

WANG, Q., ZHOU, S., WANG, L., YOU, R., YAN, S., ZHANG, Q. & LI, M. 2021. Bioactive silk fibroin scaffold with nanoarchitecture for wound healing. *Composites Part B: Engineering,* 224**,** 109165.
WANG, Y., WANG, J., HUANG, S., LIU, C. & FU, Y. 2019. Evaluating the effect of aminoglycosides on the interaction between bovine serum albumins by atomic force microscopy. *Int J Biol Macromol,* 134**,** 28-35.
ZHANG, W., CHEN, L., CHEN, J., WANG, L., GUI, X., RAN, J., XU, G., ZHAO, H., ZENG, M., JI, J., QIAN, L., ZHOU, J., OUYANG, H. & ZOU, X. 2017. Silk Fibroin Biomaterial Shows Safe and Effective Wound Healing in Animal Models and a Randomized Controlled Clinical Trial. *Adv Healthc Mater,* 6.

3. Zusammenfassung

3.1 Zusammenfassung in deutscher Sprache

Die Wundheilungsforschung beschäftigt sich seit Jahrzehnten mit der Herstellung innovativer Wundauflagen. Gerade bei orofazialen Wunden ist der Bedarf nach einer antibakteriellen Wundauflage groß. In dieser Studie wurden innovative antibakterielle Membranen auf Seidenproteinbasis für den Einsatz in der Mund-, Kiefer- und Gesichtschirurgie evaluiert. Gegossene Membranen und elektrogesponnene Vliese funktionalisiert mit Silberionen oder Gentamicin wurden auf Biokompatibilität und antibakterielle Wirksamkeit gegen typische Erreger der Mundflora untersucht. Die Oberflächenstruktur der Proben wurde mittels Rasterelektronenmikroskopie sichtbar gemacht. Die Biokompatibilität wurde anhand Zellproliferationstests, Zytotoxizitätstests und Lebend-Tot-Färbung an L929-Mausfibroblasten bewertet und die antibakterielle Testung erfolgte mittels Agardiffusionstest, Analyse der „Colony Forming Unit“ (CFU) und des qrt-PCR. Die Ergebnisse zeigten ein signifikant geringeres Koloniewachstum und eine geringere Bakterien-DNA-Zahl für Silbermembranen mit einer Verringerung der Bakterienzahl um 3 log Stufen (99,9 %) im CFU- und qrt-PCR-Assay im Vergleich zu unbehandelten Kontrollmembranen und mit Gentamicin funktionalisierten Membranen/Vliesen ($p < 0,001$). Die zweitbeste antibakterielle Wirksamkeit sowohl im CFU- als auch im qrt-PCR-Assay wiesen Gentamicinvliese auf. Zusammenfassend betrachtet, zeigten Silbermembranen eine

um 1 log Stufe bessere antibakterielle Aktivität, während Gentamicinvliese eine bessere Zytokompatibilität an L929-Zellen erbrachten. Die Daten zeigen, dass die getesteten Membranen antibakteriell sind und sich für den Einsatz in der antibakteriellen orofazialen Wundheilung eignen. Zukünftig gilt es, in vivo Versuche im Zuge eines *„proof of principle“*-Konzepts anzustreben.

3.2 Zusammenfassung in englischer Sprache

For decades, research in wound healing has been focused on the production of innovative wound dressings. Especially, due to the location and the high burden of orofacial wounds, the need for antibacterial wound dressings is rising. In this study, innovative and advanced silk protein-based antibacterial membranes were evaluated for the application in oral and maxillofacial surgery. Casted membranes and electrospun nonwovens functionalized with silver ions or Gentamicin were evaluated for biocompatibility and antibacterial activity against typical oral flora pathogens. The surface structure of the samples was visualized by scanning-electron-microscopy. Biocompatibility was evaluated by cell proliferation assays, cytotoxicity assays, and live-dead staining on L929 mouse fibroblasts, and antibacterial testing was performed by agar diffusion assay, colony forming unit (CFU) analysis, and qrt-PCR. The results showed significantly lower colony growth and bacterial DNA count for silver membranes with a reduction in bacterial count by three log-levels (99.9%) in the CFU and qrt-PCR assay compared to untreated control membranes and Gentamicin functionalized membranes/nonwovens ($p < 0.001$). Gentamicin nonwovens exhibited the second-best antibacterial efficacy in both CFU and qrt-PCR assays. In summary, silver membranes showed one log-level better antibacterial activity, whereas Gentamicin fleeces yielded higher cytocompatibility on L929 cells. The results of this study indicate the tested membranes are antibacterial and suitable for the concept of

antibacterial orofacial wound healing. Future efforts should be directed toward in vivo testing as part of a "proof of principle" approach.

4. Erklärung des Eigenanteils

Die meiner Dissertation zugrundeliegenden experimentellen Versuche wurden in den Laboren der Poliklinik für Parodontologie, Präventive Zahnmedizin und Zahnerhaltung, des Instituts für Osteologie und Biomechanik und der Klinik und Poliklinik für Mund-, Kiefer- und Gesichtschirurgie (MKG) durchgeführt.

Die getesteten Membranen und Vliese wurden von der Firma Fibrothelium GmbH hergestellt und für die Versuche dieser Studie zur Verfügung gestellt.

Der Anteil an der Publikationsdissertation ergibt sich gemäß der Autorenreihenfolge der Publikation und besteht aus der Planung und Beschreibung des Projekts, die Durchführung der Laborexperimente, welche zum Teil unter Anleitung von Herrn Frank Fischer, Dr. Philip Hartjen und Dr. Imke Fiedler erfolgten. Des Weiteren besteht der Eigenanteil an der Publikationsdissertation aus der Auswertung der Experimente, die Literaturrecherche für die Publikation sowie das Schreiben und die Entstehung der Publikation selbst.

5. Danksagung

Ich möchte mich zuallererst bei meinen Eltern Kiana und Michael Schäfer für Ihre bedingungslose Liebe und Unterstützung bedanken.

Weiterhin danke ich Herrn Prof. Dr. Dr. Ralf Smeets für die Überlassung dieser Arbeit, die Betreuung und Inspiration. Danke Ihnen für die jahrelange Förderung und Unterstützung.

Auch möchte ich mich herzlichst bei Dr. Ulrike Peters, Herrn Frank Fischer und Dr. Philip Hartjen für die Zeit und Mühe im Labor und darüber hinaus bedanken.

Zuletzt bedanke ich mich bei Herrn Prof. Dr. Dr. Thomas Beikler für die freundliche Aufnahme und die Möglichkeit, meine Forschungsarbeiten im Zahnkliniklabor durchzuführen, und bei Herrn Prof. Dr. Dr. Martin Gosau für die Aufnahme und Integration in das Team der Klinik und Poliklinik für Mund-, Kiefer- und Gesichtschirurgie am Universitätsklinikum Hamburg-Eppendorf.

6. Lebenslauf

Persönliche Daten:

Geboren am 18. August 1996 in Shiraz, Iran

Schulbildung:

09/2008 – 09 2010 Kaiser-Wilhelm- und Ratsgymnasium Hannover
09/2010 – 06/2016 Altes Gymnasium Flensburg
30.06.2016 Allgemeine Hochschulreife

Hochschulbildung und berufliche Ausbildung:

10/2016 – 12/2022 Studium der Medizin an der Universität Hamburg, Medizinische Fakultät, Universitätsklinikum Hamburg-Eppendorf

Famulaturen und Praktisches Jahr:

08/2019 - 09/2019 Famulatur in der Praxis für Plastische Chirurgie & Hals-Nasen-Ohren-Heilkunde, Dr. Eckert Knoche, Hamburg
09/2019 - 10/2019 Famulatur an der Klinik und Polyklinik für Mund-, Kiefer- und Gesichtschirurgie, Universitätsklinikum Hamburg-Eppendorf
11/2021 - 03/2022 MPJ (Tertial Innere Medizin) an der Mbarara University of Science and Technology, Mbarara
03/2022 - 06/2022 MPJ (Tertial Allgemeinchirurgie) Israelitisches Krankenhaus Hamburg
06/2022 - 08/2022 MPJ (Tertial Wahlfach) an der Klinik für Schädel-, Kiefer- und Gesichtschirurgie Universitäätsspital Bern, Schweiz
08/2022 - 10/2022 MPJ (Tertial Wahlfach) an Klinik und Polyklinik für Mund-, Kiefer- und Gesichtschirurgie, Universitätsklinikum Hamburg-Eppendorf
07/2019 - heute Wissenschaftliche Mitarbeiterin an der Klinik und Polyklinik für Mund-, Kiefer- und Gesichtschirurgie, Universitätsklinikum Hamburg-Eppendorf

Freiwilligenarbeit:

01/2019 - heute Creative Change e.V., Offenbach, Deutschland; Tätigkeit: Leitung von theaterpädagogischen Projekten bundesweit an Schulen mit dem Ziel der Persönlichkeitsförderung und Stärkung der politischen Bildung von Kindern und Jugendlichen.
11/2021 - 03/2022 McNeil Medical Center at Uganda Lodge (NGO) Ruhanga, Uganda; Tätigkeit: Medizinischer Freiwilliger, Unterstützung bei der Etablierung von medizinischen Einsätzen im ruralen West-Uganda.
03/2022 - heute Mbarara University of Science and Technology, Mbarara, Uganda; Tätigkeit: Koordinatorin des Studentenaustauschprogramms

6.1 Publikationen

Gehrke P, Hartjen P, Smeets R, Gosau M, Peters U, Beikler T, Fischer C, Stolzer C, Geis-Gerstorfer J, Weigl P, *__Schäfer S.__ Marginal Adaptation and Microbial Leakage at Conometric Prosthetic Connections for Implant-Supported Single Crowns: An In Vitro Investigation. Int J Mol Sci. 2021 Jan 17;22(2):881. doi: 10.3390/ijms22020881. PMID: 33477311; PMCID: PMC7830972.

***Schäfer S**, Al-Qaddo H, Gosau M, Smeets R, Hartjen P, Friedrich RE, Nada OA, Vollkommer T, Rashad A. Cytocompatibility of Bone Substitute Materials and Membranes. In Vivo. 2021 Jul-Aug;35(4):2035-2040. doi: 10.21873/invivo.12472. PMID: 34182478; PMCID: PMC8286533.

Gehrke P, Burg S, Peters U, Beikler T, Fischer C, Rupp F, Schweizer E, Weigl P, Sader R, Smeets R, **Schäfer S**. Bacterial translocation and microgap formation at a novel conical indexed implant abutment system for single crowns. Clin Oral Investig. 2022 Feb;26(2):1375-1389. doi: 10.1007/s00784-021-04112-2. Epub 2021 Aug 16. PMID: 34401947; PMCID: PMC8816325.

***Schäfer S**, Smeets R, Köpf M, Drinic A, Kopp A, Kröger N, Hartjen P, Assaf AT, Aavani F, Beikler T, Peters U, Fiedler I, Busse B, Stürmer EK, Vollkommer T, Gosau M, Fuest S. Antibacterial properties of functionalized silk fibroin and sericin membranes for wound healing applications in oral and maxillofacial surgery. Biomater Adv. 2022 Apr;135:212740. doi: 10.1016/j.bioadv.2022.212740. Epub 2022 Mar 17. PMID: 35929202.

Smeets R, Henningsen A, Zernial O, Stürmer E, Fiedler I, **Schäfer S**, Gosau M, Gaudin R, Stolzer C, Reinelt A, Fuest S. New and innovative biomaterials, techniques and therapy concepts: Biologization in maxillofacial surgery, oral surgery and dentistry is in full swing. PRF, PRGF, PRP, blood plasma-stabilized augmentations, supplementation of micronutrients and vitamins - what opportunities do such "biological" approaches actually offer? We introduce them here. GMS Interdiscip Plast Reconstr Surg DGPW. 2022 Jul 5;11:Doc05. doi: 10.3205/iprs000166. PMID: 35909817; PMCID: PMC9285113.

***Schäfer S**, Aavani F, Köpf M, Drinic A, Stürmer EK, Fuest S, Grust ALC, Gosau M, Smeets R. Silk proteins in reconstructive surgery: Do they possess an inherent

antibacterial activity? A systematic review. Wound Repair Regen. 2022 Sep 15. doi: 10.1111/wrr.13049. Epub ahead of print. PMID: 36106818.

*Korrespondierender Autor

7. Eidesstattliche Erklärung

Ich versichere ausdrücklich, dass ich die Arbeit selbständig und ohne fremde Hilfe verfasst, andere als die von mir angegebenen Quellen und Hilfsmittel nicht benutzt und die aus den benutzten Werken wörtlich oder inhaltlich entnommenen Stellen einzeln nach Ausgabe (Auflage und Jahr des Erscheinens), Band und Seite des benutzten Werkes kenntlich gemacht habe.
Ferner versichere ich, dass ich die Dissertation bisher nicht einem Fachvertreter an einer anderen Hochschule zur Überprüfung vorgelegt oder mich anderweitig um Zulassung zur Promotion beworben habe. Ich erkläre mich einverstanden, dass meine Dissertation vom Dekanat der Medizinischen Fakultät mit einer gängigen Software zur Erkennung von Plagiaten überprüft werden kann.

Unterschrift: .....